

Local weak form meshless techniques based on the radial point interpolation (RPI) method and local boundary integral equation (LBIE) method to evaluate European and American options

Jamal Amani Rad^a, Kourosh Parand^a, Saeid Abbasbandy^{b,*}

^a*Department of Computer Sciences, Faculty of Mathematical Sciences, Shahid Beheshti University, Evin, P.O. Box 198396-3113, Tehran, Iran*

^b*Department of Mathematics, Imam Khomeini International University, Ghazvin 34149-16818, Iran*

Abstract

For the first time in mathematical finance field, we propose the local weak form meshless methods for option pricing; especially in this paper we select and analysis two schemes of them named local boundary integral equation method (LBIE) based on moving least squares approximation (MLS) and local radial point interpolation (LRPI) based on Wu's compactly supported radial basis functions (WCS-RBFs). LBIE and LRPI schemes are the truly meshless methods, because, a traditional non-overlapping, continuous mesh is not required, either for the construction of the shape functions, or for the integration of the local sub-domains. In this work, the American option which is a free boundary problem, is reduced to a problem with fixed boundary using a Richardson extrapolation technique. Then the θ -weighted scheme is employed for the time derivative. Stability analysis of the methods is analyzed and performed by the matrix method. In fact, based on an analysis carried out in the present paper, the methods are unconditionally stable for implicit Euler ($\theta = 0$) and Crank-Nicolson ($\theta = 0.5$) schemes. It should be noted that LBIE and LRPI schemes lead to banded and sparse system matrices. Therefore, we use a powerful iterative algorithm named the Bi-conjugate gradient stabilized method (BCGSTAB) to get rid of this system. Numerical experiments are presented showing that the LBIE and LRPI approaches are extremely accurate and fast.

Keywords: Option Pricing; American option; Meshless weak form; LBIE; MLS; LRPI; Richardson Extrapolation; BCGSTAB; Stability analysis.

AMS subject classification: 91G80; 91G60; 35R35.

1. Introduction

Over the last thirty years, financial derivatives have raised increasing popularity in the markets. In particular, large volumes of options are traded everyday all over the world and it is therefore of great importance to give a correct valuation of these instruments.

Options are contracts that give to the holder the right to buy (call) or to sell (put) an asset (underlying) at a previously agreed price (strike price) on or before a given expiration date (maturity). The majority of options can be grouped in two categories: European options, which can be exercised only at maturity, and American options, which can be exercised not only at maturity but also at any time prior to maturity.

Options are priced using mathematical models that are often challenging to solve. In particular, the famous Black-Scholes model [1] yields explicit pricing formulae for some kinds of European options, including vanilla call and put, but the modeling of American options is quite complicated. Hence, an analytical solution is impossible. Therefore, to solve this problem, we need to have a powerful computational method. To this aim, the most common approaches are the finite difference/finite element/finite volume methods/fast Fourier transform (see, e.g., [2, 3, 4, 5, 6, 7, 8, 9, 10, 11, 12, 13, 14, 15, 16, 17, 18, 19]) and the binomial/trinomial

*Corresponding author

Email addresses: j.amanirad@gmail.com; j_amanirad@sbu.ac.ir (Jamal Amani Rad), k_parand@sbu.ac.ir (Kourosh Parand), abbasbandy@yahoo.com (Saeid Abbasbandy)

trees (see, e.g., [20, 21, 22, 23]), nevertheless some authors have also proposed the use of meshless algorithms based on radial basis functions [24, 25, 26, 27, 28, 29] and on quasi radial basis functions [30].

Recently, a great attention has been paid to the development of various meshless formulations for solution of boundary value problems in many branches of science and engineering. Meshless methods are becoming viable alternatives to either finite element method (FEM) and boundary element method (BEM). Compared to the FEM and the BEM, the key feature of this kind of method is the absence of an explicit mesh, and the approximate solutions are constructed entirely based on a group of scattered nodes. Meshless methods have been found to possess special advantages on problems to that the conventional mesh-based methods are difficult to be applied. These generally include problems with complicated boundary, moving boundary and so on [31, 32, 33, 34, 35, 36, 37]. A lot of meshless methods are based on a weak-form formulation on global domain or a set of local sub-domains.

In the global formulation background cells are needed for the integration of the weak form. Strictly speaking, these meshless methods are not truly meshless methods. It must be realized that integration is completed only those background cells with a nonzero shape function.

In the financial literature global meshless method (or Kansa method) has been proposed for pricing options under various models such as the Black-Scholes model, stochastic volatility models and Merton models with jumps. In particular, in the case of Black-Scholes model, we mention two papers by Hon and his co-author [30, 26] where the global RBFs and quasi-radial basis functions are developed. Moreover, as regards the cases of stochastic volatility models and Black-Scholes model on two underlying assets, new global meshless method is presented in Ballestra and Pacelli [25]. The techniques presented in [25] is combined of the Gaussian radial basis functions with a suitable operator splitting scheme. Also a numerical method has recently been presented by Saib et al. [38]. In particular, in this latter work, a differential quadrature radial basis functions is used to reduce the American option pricing problem under Merton's jump-diffusion model to a system of ordinary differential equations. The interested reader can also see [39, 40].

In methods based on local weak-form formulation no cells are needed and therefore they are often known as truly meshless methods. By using a simple form for the geometry of the sub-domains, one can use a numerical integration method, easily. Recently, two family of meshless methods, on the basis of the local weak form for arbitrary partial differential equations with moving least-square (MLS) and radial basis functions (RBFs) approximation have been developed [41, 42, 43, 44, 45]. Local boundary integral equation method (LBIE) with moving least squares approximation and local radial point interpolations (LRPI) with radial basis functions have been developed by Zhu et al. [46] and Liu et al. [47, 48], respectively. Both methods (LBIE and LRPI) are meshless, as no domain/boundary traditional non-overlapping meshes are required in these two approaches. Particularly, the LRPI meshless method reduces the problem dimension by one, has shape functions with delta function properties, and expresses the derivatives of shape functions explicitly and readily. Thus it allows one to easily impose essential boundary and initial (or final) conditions. Though the LBIE method is an efficient meshless method, it is difficult to enforce the essential boundary conditions for that the shape function constructed by the moving least-squares (MLS) approximation lacks the delta function property. Some special techniques have to be used to overcome the problem, for example, the Lagrange multiplier method and the penalty method [49]. In this paper, meshless collocation method is applied to the nodes on the boundaries. The papers of Zhu et al. [46, 50, 51] in linear and non-linear acoustic and potential problems, and for heat conduction problems, the works of Sladek brothers [52, 53] by meshless LBIE are useful for researchers. This method has now been successfully extended to a wide rang of problems in engineering. For some examples of these problems, see [54, 55, 56] and other references therein. The interested reader of meshless methods can also see [57, 58].

The objective of this paper is to extend the LRPI based on Wu's compactly supported radial basis functions (WCS-RBFs) with C^4 smoothness [59] and LBIE method based on moving least squares with cubic spline weight function to evaluate European and American options. To the best of our knowledge, the local weak form of meshless method has not yet been used in mathematical finance. Therefore, it appears to be interesting to extend such a numerical technique also to option valuation, which is done in the present manuscript. In particular, we develop a local weak form meshless algorithm for pricing both European and American options under the Black-Scholes model.

In addition, in this paper the infinite space domain is truncated to $[0, S_{max}]$ with a sufficiently large S_{max} to avoid an unacceptably large truncation error. The options' payoffs considered in this paper are non-smooth functions, in particular their derivatives are discontinuous at the strike price. Therefore, to

reduce as much as possible the losses of accuracy the points of the trial functions are concentrated in a spatial region close to the strike prices. So, we employ the change of variables proposed by Clarke and Parrott [60].

As far as the time discretization is concerned, we use the θ -weighted scheme. Stability analysis of the method is analyzed and performed by the matrix method in the present paper. Furthermore, in this paper we will see that the time semi-discretization is unconditionally stable for implicit Euler ($\theta = 0$) and Crank-Nicolson ($\theta = 0.5$) schemes.

Finally, in order to solve the free boundary problem that arises in the case of American options is computed by Richardson extrapolation of the price of Bermudan option. In essence the Richardson extrapolation reduces the free boundary problem and linear complementarity problem to a fixed boundary problem which is much simpler to solve.

The paper is organized as follows: In Section 2 a detailed description of the Black-Scholes model for European and American options is provided. Section 3 is devoted to presenting the LBIE and LRPI approaches and the application of such a numerical technique to the option pricing problems considered is shown in this section. The numerical results obtained are presented and discussed in Section 4 and finally, in Section 5, some conclusions are drawn.

2. The Black-Scholes model for European and American options

For the sake of simplicity, from now we restrict our attention to options of put type. However the reader will note that the numerical method presented in this paper can be used with little modifications also to price call options.

Let us consider a put option with maturity T and strike price E on an underlying asset s that follows (under the risk-neutral measure) the stochastic differential equation [61]:

$$ds = r s dt + \sigma s dW, \quad (2.1)$$

where r and σ are the interest rate and the volatility, respectively. Moreover let $V(s, t)$ denote the option price, and let us define the Black-Scholes operator [61]:

$$\mathcal{L}V(s, t) = -\frac{\partial}{\partial t}V(s, t) - \frac{\sigma^2}{2}s^2\frac{\partial^2}{\partial s^2}V(s, t) - rs\frac{\partial}{\partial s}V(s, t) + rV(s, t). \quad (2.2)$$

2.1. European option

The option price $V(s, t)$ satisfies, for $s \in (0, +\infty)$ and $t \in [0, T)$, the following partial differential problem [61, 30, 26]:

$$\mathcal{L}V(s, t) = 0, \quad (2.3)$$

with final condition:

$$V(s, T) = \varsigma(s), \quad (2.4)$$

and boundary conditions:

$$V(0, t) = E \exp\{-r(T - t)\}, \quad \lim_{s \rightarrow +\infty} V(s, t) = 0, \quad (2.5)$$

where ς is the so-called option's payoff:

$$\varsigma(s) = \max(E - s, 0), \quad (2.6)$$

which is clearly not differentiable at $s = E$.

An exact analytical solution to the problem (2.3)-(2.5), i.e. the famous Black-Scholes formula, is available.

2.2. American option

The option price $V(s, t)$ satisfies, for $s \in [0, +\infty)$ and $t \in [0, T)$, the following partial differential problem [30, 26]:

$$\mathcal{L}V(s, t) = 0, \quad s > B(t), \quad (2.7)$$

$$V(s, t) = E - s, \quad 0 \leq s < B(t), \quad (2.8)$$

$$\left. \frac{\partial V(s, t)}{\partial s} \right|_{s=B(t)} = -1, \quad (2.9)$$

$$V(B(t), t) = E - B(t), \quad (2.10)$$

with final condition:

$$V(s, T) = \varsigma(s), \quad (2.11)$$

and boundary condition:

$$\lim_{s \rightarrow +\infty} V(s, t) = 0, \quad (2.12)$$

where $B(t)$ denotes the so-called exercise boundary, which is unknown and is implicitly defined by (2.7)-(2.12). The above free-boundary partial differential problem does not have an exact closed-form solution, and thus some numerical approximation is required.

Problem (2.7)-(2.12) can be reformulated as a linear complementarity problem [10]:

$$\mathcal{L}V(s, t) \geq 0, \quad (2.13)$$

$$V(s, t) - \varsigma(s) \geq 0, \quad (2.14)$$

$$(\mathcal{L}V(s, t)) \cdot (V(s, t) - \varsigma(s)) = 0, \quad (2.15)$$

which holds for $s \in (0, +\infty)$ and $t \in [0, T)$, with final condition:

$$V(s, T) = \varsigma(s), \quad (2.16)$$

and boundary conditions:

$$V(0, t) = E, \quad \lim_{s \rightarrow +\infty} V(s, t) = 0. \quad (2.17)$$

In this work, the price of American option is computed by Richardson extrapolation of the price of Bermudan option which is also employed in other works, such as for example [8, 9, 23, 25, 62]. In essence the Richardson extrapolation reduces the free boundary problem and linear complementarity problem to a fixed boundary problem which is much simpler to solve. Thus, instead of describing the aforementioned linear complementarity problem or penalty method, we directly focus our attention onto the partial differential equation satisfied by the price of a Bermudan option which is faster and more accurate than other methods. Let us consider in the interval $[0, T]$, $M + 1$ equally spaced time levels $t_0 = 0, t_1, t_2, \dots, t_M = T$. Let $V_M(s, t)$ denote the price of a Bermudan option with maturity T and strike price E . The Bermudan option is an option that can be exercised not on the whole time interval $[0, T]$, but only at the dates t_0, t_1, \dots, t_M . That is we consider the problems

$$\begin{cases} \mathcal{L}V_M(s, t) = 0, \\ V_M(0, t) = E, \end{cases} \quad \lim_{s \rightarrow \infty} V_M(s, t) = 0, \quad (2.18)$$

which hold in the time intervals $(t_0, t_1), (t_1, t_2), \dots, (t_{M-1}, t_M)$. By doing that also the relation (2.15) is automatically satisfied in every time interval (t_k, t_{k+1}) , $k = 0, 1, \dots, M - 1$. Moreover, the relation (2.14) is enforced only at times t_0, t_1, \dots, t_{M-1} , by setting

$$V_M(s, t_k) = \max(\lim_{t \rightarrow t_k^+} V_M(s, t), \varsigma(s)), \quad k = 0, 1, \dots, M - 1. \quad (2.19)$$

Note that the function $V_M(\cdot, t_k)$ computed according to (2.19) is used as the final condition for the problem (2.18) that holds in the time interval (t_{k-1}, t_k) , $k = 1, 2, \dots, M-1$. Instead, the final condition for the problem (2.18) that holds in the time interval (t_{M-1}, t_M) , according to the relation (2.16), is prescribed as follows:

$$V_M(s, t_M) = \varsigma(s). \quad (2.20)$$

That is, in summary, problems (2.18) are recursively solved for $k = M-1, M-2, \dots, 0$, starting from the condition (2.20), and at each time $t_{M-1}, t_{M-2}, \dots, t_0$ the American constraint (2.19) is imposed.

The Bermudan option price $V_M(s, t)$ tends to become a fair approximation of the American option price $V(s, t)$ as the number of exercise dates M increases. In this work the accuracy of $V_M(s, t)$ is enhanced by Richardson extrapolation which is second-order accurate in time.

3. Methodology

To evaluate the option, the LBIE and LRPI methods are used in the present work. The methods are based on local weak forms over intersecting sub-domains. For ease of exposition, we focus our attention onto American option, as the application of the method to European option is substantially analogous and requires only minor modifications. At first we discuss a time-stepping method for the time derivative.

3.1. Time discretization

First of all, we discretize the Black-Scholes operator (2.2) in time. For this propose, we can apply the Laplace transform or use a time-stepping approximation. Algorithms for the numerical inversion of a Laplace transform lead to a reduction in accuracy. Then, we employ a time-stepping method to overcome the time derivatives in this equation.

Let $V^k(s)$ denote a function approximating $V_M(s, t_k)$, $k = 0, 1, \dots, M-1$. Note that the subscript M has been removed from $V^k(s)$ to keep the notation simple. According to (2.20) we set $V^M(s) = \varsigma(s)$. Let us consider the following θ -weighted scheme:

$$\begin{aligned} \mathcal{L}V^k(s) = & \frac{\theta\sigma^2}{2}s^2\frac{d^2}{ds^2}V^{k+1}(s) + \theta rs\frac{d}{ds}V^{k+1}(s) + (-\theta r + \frac{1}{\Delta t})V^{k+1}(s) - \\ & \frac{(\theta-1)\sigma^2}{2}s^2\frac{d^2}{ds^2}V^k(s) - (\theta-1)rs\frac{d}{ds}V^k(s) - \\ & (-\theta-1)r + \frac{1}{\Delta t})V^k(s). \end{aligned} \quad (3.1)$$

Therefore, the American option problems are rewritten as follows:

$$\begin{cases} \mathcal{L}V^k(s) = 0, \\ V^k(0) = E, \quad \lim_{s \rightarrow \infty} V^k(s) = 0, \end{cases} \quad (3.2)$$

and also, the relations (2.19) and (2.20) are rewritten as follows:

$$\begin{aligned} V^k(s) &= \max \left(\lim_{t \rightarrow t_{k+1}^+} V^k(s), \varsigma(s) \right), \quad k = 0, 1, \dots, M-1, \\ V^M(s) &= \varsigma(s). \end{aligned} \quad (3.3)$$

3.2. Spatial variable transformation

Now, the infinite space domain is truncated to $[0, S_{max}]$ with a sufficiently large S_{max} to avoid an unacceptably large truncation error. However, in [63] shown that upper bound of the asset price is three or four times of the strike price, so we can set $S_{max} = 5E$. The options' payoffs considered in this paper are non-smooth functions, in particular their derivatives are discontinuous at the strike price. Therefore, to reduce the losses of accuracy the points of the trial functions are concentrated in a spatial region close to

$s = E$. So, we employ the following change of variables which is not new but has already been proposed by [60] and has also been employed for example in [25, 39, 40]:

$$x(s) = \frac{\sinh^{-1}(\xi(s - E)) + \sinh^{-1}(\xi E)}{\sinh^{-1}(\xi(S_{max} - E)) + \sinh^{-1}(\xi E)}, \quad (3.4)$$

or

$$s(x) = \frac{1}{\xi} \sinh \left(x \sinh^{-1}(\xi(S_{max} - E)) - (1 - x) \sinh^{-1}(\xi E) \right) + E. \quad (3.5)$$

Note that the Eq. (3.4) maps the $[0, S_{max}]$ to the $[0, 1]$. We define

$$U(x, t) = V(s(x), t), \quad (3.6)$$

$$\begin{aligned} \tilde{\mathcal{L}}U^k(x) &= \theta\alpha(x)\frac{d^2}{dx^2}U^{k+1}(x) + \theta\beta(x)\frac{d}{dx}U^{k+1}(x) + \gamma_1U^{k+1}(x) - \\ &\quad (\theta - 1)\alpha(x)\frac{d^2}{dx^2}U^k(x) - (\theta - 1)\beta(x)\frac{d}{dx}U^k(x) - \gamma_2U^k(x), \end{aligned} \quad (3.7)$$

where

$$\begin{aligned} \alpha(x) &= \frac{1}{2}\sigma^2 \left(\frac{s(x)}{s'(x)} \right)^2, \\ \beta(x) &= -\frac{1}{2}\sigma^2 \left(\frac{s(x)}{s'(x)} \right)^2 \frac{s''(x)}{s'(x)} + r \frac{s(x)}{s'(x)}, \\ \gamma_1 &= \left(-\theta r + \frac{1}{\Delta t} \right), \\ \gamma_2 &= \left(-(\theta - 1)r + \frac{1}{\Delta t} \right). \end{aligned}$$

Using the change of variable (3.4), the relations (3.2) are rewritten as follows:

$$\begin{cases} \tilde{\mathcal{L}}U^k(x) = 0, \\ U^k(0) = E, \quad U^k(1) = 0, \end{cases} \quad (3.8)$$

and also, the relations (3.3) are rewritten as follows:

$$\begin{aligned} U^k(x) &= \max(\lim_{t \rightarrow t_{k+1}^+} U^k(x), \tilde{\zeta}(x)), \quad k = 0, 1, \dots, M - 1, \\ U^M(x) &= \tilde{\zeta}(x), \end{aligned} \quad (3.9)$$

where

$$\tilde{\zeta}(x) = \max(E - s(x), 0). \quad (3.10)$$

3.3. The local weak form

In this section, we use the local weak form instead of the global weak form. The LBIE and LRPI methods construct the weak form over local sub-domains such as Ω_s , which is a small region taken for each node in the global domain $\Omega = [0, 1]$. The local sub-domains overlap each other and cover the whole global domain Ω . This local sub-domains could be of any size. Therefore the local weak form of the approximate equation (3.8) for $x \in \Omega_s^i$ can be written as

$$\begin{aligned} &\int_{\Omega_s^i} \left(\theta\alpha(x)\frac{d^2}{dx^2}U^{k+1}(x) + \theta\beta(x)\frac{d}{dx}U^{k+1}(x) + \gamma_1U^{k+1}(x) \right) u^* d\Omega \\ &= \int_{\Omega_s^i} \left((\theta - 1)\alpha(x)\frac{d^2}{dx^2}U^k(x) + (\theta - 1)\beta(x)\frac{d}{dx}U^k(x) + \gamma_2U^k(x) \right) u^* d\Omega, \end{aligned} \quad (3.11)$$

which Ω_s^i is the local domain associated with the point i , i.e. it is a interval centered at x of radius r_Q . In LRPI, u^* is the Heaviside step function

$$u^*(x) = \begin{cases} 1, & x \in \Omega_s^i, \\ 0, & \text{otherwise,} \end{cases}$$

as the test function in each local domain, but in LBIE method, u^* is the fundamental solution for the one-dimensional Laplace operator defined by the equation

$$\frac{\partial^2}{\partial x^2} u^*(x, \xi) = \delta(x, \xi), \quad (3.12)$$

where x and ξ are a field point and a source point, respectively, and δ is Dirac delta function. The fundamental solution and its derivative are given as follows

$$u^*(x, \xi) = \frac{1}{2}|x - \xi|, \quad (3.13)$$

$$\frac{\partial}{\partial x} u^*(x, \xi) = \frac{1}{2} \text{sgn}(x - \xi),$$

where the symbol sgn denotes the signum function. Using the integration by parts, we have

$$\begin{aligned} \int_{\Omega_s^i} \alpha(x) \frac{d^2}{dx^2} U^j(x) u^* d\Omega &= \left(\alpha(x) \frac{d}{dx} U^j(x) - \alpha'(x) U^j(x) \right) u^* \Big|_{\partial\Omega_s^i} \\ &+ \int_{\Omega_s^i} U^j(x) \alpha''(x) u^* d\Omega + \int_{\Omega_s^i} U^j(x) \alpha'(x) \frac{\partial u^*}{\partial x} d\Omega - \int_{\Omega_s^i} \frac{d}{dx} U^j(x) \alpha(x) \frac{\partial u^*}{\partial x} d\Omega, \end{aligned} \quad (3.14)$$

and

$$\begin{aligned} \int_{\Omega_s^i} \beta(x) \frac{d}{dx} U^j(x) u^* d\Omega &= \beta(x) U^j(x) u^* \Big|_{\partial\Omega_s^i} - \int_{\Omega_s^i} U^j(x) \beta'(x) u^* d\Omega \\ &- \int_{\Omega_s^i} U^j(x) \beta(x) \frac{\partial u^*}{\partial x} d\Omega, \end{aligned} \quad (3.15)$$

for $j = k, k + 1$. In above relations, $\partial\Omega_s^i$ is the boundary of Ω_s^i . Using relations (3.11), (3.12), (3.14) and (3.15) for LBIE scheme, we get

$$\begin{aligned}
& \left. \frac{\theta}{2} |x - x^i| \left(\alpha(x) \frac{d}{dx} U^{k+1}(x) - \alpha'(x) U^{k+1}(x) \right) \right|_{\partial\Omega_s^i} \\
& + \frac{\theta}{2} \int_{\Omega_s^i} U^{k+1}(x) \alpha''(x) |x - x^i| d\Omega + \frac{\theta}{2} |x - x^i| \beta(x) U^{k+1}(x) \Big|_{\partial\Omega_s^i} \\
& - \frac{\theta}{2} \int_{\Omega_s^i} U^{k+1}(x) \beta'(x) |x - x^i| d\Omega \\
& + \gamma_1 \int_{\Omega_s^i} U^{k+1}(x) d\Omega - \frac{\theta}{2} \int_{\Omega_s^i} U^{k+1}(x) \beta(x) \operatorname{sgn}(x - x^i) d\Omega \\
& + \frac{\theta}{2} \int_{\Omega_s^i} U^{k+1}(x) \alpha'(x) \operatorname{sgn}(x - x^i) d\Omega - \frac{\theta}{2} \int_{\Omega_s^i} \frac{d}{dx} U^{k+1}(x) \alpha(x) \operatorname{sgn}(x - x^i) d\Omega \\
& = \frac{\theta - 1}{2} |x - x^i| \left(\alpha(x) \frac{d}{dx} U^k(x) - \alpha'(x) U^k(x) \right) \Big|_{\partial\Omega_s^i} \\
& + \frac{\theta - 1}{2} \int_{\Omega_s^i} U^k(x) \alpha''(x) |x - x^i| d\Omega + \frac{\theta - 1}{2} |x - x^i| \beta(x) U^k(x) \Big|_{\partial\Omega_s^i} \\
& - \frac{\theta - 1}{2} \int_{\Omega_s^i} U^k(x) \beta'(x) |x - x^i| d\Omega + \gamma_1 \int_{\Omega_s^i} U^k(x) d\Omega \\
& - \frac{\theta - 1}{2} \int_{\Omega_s^i} U^k(x) \beta(x) \operatorname{sgn}(x - x^i) d\Omega + \frac{\theta - 1}{2} \int_{\Omega_s^i} U^k(x) \alpha'(x) \operatorname{sgn}(x - x^i) d\Omega \\
& - \frac{\theta - 1}{2} \int_{\Omega_s^i} \frac{d}{dx} U^k(x) \alpha(x) \operatorname{sgn}(x - x^i) d\Omega. \tag{3.16}
\end{aligned}$$

Also, because the derivative of the Heaviside step function u^* is equal to zero, then for LRPI scheme using relations (3.14) and (3.15) the local weak form equation (3.11) is transformed into the following simple local integral equation

$$\begin{aligned}
& \left. \theta \left(\alpha(x) \frac{d}{dx} U^{k+1}(x) - \alpha'(x) U^{k+1}(x) \right) \right|_{\partial\Omega_s^i} \\
& + \theta \int_{\Omega_s^i} U^{k+1}(x) \alpha''(x) d\Omega + \theta \beta(x) U^{k+1}(x) \Big|_{\partial\Omega_s^i} - \theta \int_{\Omega_s^i} U^{k+1}(x) \beta'(x) d\Omega \\
& + \gamma_1 \int_{\Omega_s^i} U^{k+1}(x) d\Omega \\
& = (\theta - 1) \left(\alpha(x) \frac{d}{dx} U^k(x) - \alpha'(x) U^k(x) \right) \Big|_{\partial\Omega_s^i} \\
& + (\theta - 1) \int_{\Omega_s^i} U^k(x) \alpha''(x) d\Omega + (\theta - 1) \beta(x) U^k(x) \Big|_{\partial\Omega_s^i} - (\theta - 1) \int_{\Omega_s^i} U^k(x) \beta'(x) d\Omega \\
& + \gamma_2 \int_{\Omega_s^i} U^k(x) d\Omega. \tag{3.17}
\end{aligned}$$

It is important to observe that in relations (3.16) and (3.17) exist unknown functions, we should approximate these functions. To this aim the local integral equations (3.16) and (3.17) are transformed in to a system of algebraic equations with real unknown quantities at nodes used for spatial approximation, as described in the next section.

3.4. Spatial approximation

Instead of using traditional non-overlapping, contiguous meshes to form the interpolation scheme, the LBIE and LRPIM methods use a local interpolation or approximation to represent the trial or test functions with the values (or the fictitious values) of the unknown variable at some randomly located nodes. There are a number of local interpolation schemes for this purpose. The moving least squares approximation and radial point interpolation are two of them. In this section, the fundamental idea of these approximations is reviewed.

3.4.1. The MLS approximation

Consider a sub-domain Ω_x of Ω in the neighborhood of a point x for the definition of the MLS approximation of the trial function around x . To approximate the distribution of function $U^k(x)$ in Ω_x , over a number of randomly located nodes $\{x^i\}$, $i = 1, 2, \dots, n$, the moving least squares approximation $\tilde{U}^k(x)$ of $U^k(x)$ for each $x \in \Omega_x$, can be defined by [49, 50, 51, 52, 54, 64, 65]

$$\tilde{U}^k(x) = \mathbf{p}^T(x) \mathbf{a}^k(x), \quad \forall x \in \Omega_x, \quad (3.18)$$

where $\mathbf{p}^T(x) = [p_1(x) \ p_2(x) \ \dots \ p_m(x)]$ is a complete monomial basis of order m . In the present work, both the constant and the linear monomials are used, i.e. we set $m = 2$. Also $\mathbf{a}^k(x)$ is an undetermined coefficient vector with components $a_j^k(x)$, $j = 1, 2, \dots, m$, which is decided by minimizing the evaluation function $\mathbf{J}^k(x)$ shown below [49, 50, 51, 52, 54, 64, 65]

$$\begin{aligned} \mathbf{J}^k(x) &= \sum_{i=1}^n w_i(x) \left[\mathbf{p}^T(x^i) \mathbf{a}^k(x) - \hat{U}_i^k \right]^2 \\ &= \left[\mathbf{P} \mathbf{a}^k(x) - \hat{\mathbf{U}}^k \right]^T \cdot \mathbf{W} \cdot \left[\mathbf{P} \mathbf{a}^k(x) - \hat{\mathbf{U}}^k \right], \end{aligned} \quad (3.19)$$

where $w_i(x)$ is a positive weight function associated with the node i , which decreases as $|x - x_i|$ increases. It always takes unit value at the sampling point x and vanishes outside the support domain Ω_x of x . The cubic spline weight function is considered in the present work. The weight function corresponding to node i for a one-dimensional domain may be written as [49, 50, 51]

$$w_i(x) = \begin{cases} \frac{2}{3} - 4r_i^2 + 4r_i^3, & r_i \leq 0.5, \\ \frac{4}{3} - 4r_i + 4r_i^2 - \frac{4}{3}r_i^3, & 0.5 < r_i \leq 1, \\ 0, & r_i > 1, \end{cases} \quad (3.20)$$

where $r_i = |x - x_i|/r_w$ is the distance from node x_i to x , while r_w is the size of support for the weight function $w_i(x)$.

In relation (3.19), n is the number of nodes in the support domain Ω_x and \hat{U}_i^k are the fictitious nodal nodes. The matrices \mathbf{P} and \mathbf{W} are defined as [49, 50, 51, 52, 54, 64, 65]

$$\mathbf{P} = \begin{bmatrix} \mathbf{p}^T(x^1) \\ \mathbf{p}^T(x^2) \\ \vdots \\ \mathbf{p}^T(x^n) \end{bmatrix}_{n \times m}, \quad \mathbf{W} = \text{Diag}(w_1(x), w_2(x), \dots, w_n(x)). \quad (3.21)$$

The stationarity condition of $\mathbf{J}^k(x)$ in Eq. (3.19) with respect to $\mathbf{a}^k(x)$ i.e. $\partial \mathbf{J}^k(x) / \partial \mathbf{a}^k(x)$, leads to the following linear relation between $\mathbf{a}^k(x)$ and $\hat{\mathbf{U}}^k$ (see [49, 50, 51, 52, 54, 64, 65] for more details)

$$\mathbf{A}(x) \mathbf{a}^k(x) = \mathbf{B}(x) \hat{\mathbf{U}}^k, \quad (3.22)$$

from which

$$\mathbf{a}^k(x) = \mathbf{A}^{-1}(x) \mathbf{B}(x) \hat{\mathbf{U}}^k, \quad (3.23)$$

where the matrices $\mathbf{A}(x)$ and $\mathbf{B}(x)$ are defined by

$$\mathbf{B}(x) = \mathbf{P}^T \mathbf{W}, \quad \mathbf{A}(x) = \mathbf{P}^T \mathbf{W} \mathbf{P} = \mathbf{B}(x) \mathbf{P}.$$

The MLS is well-defined only when \mathbf{A} is non-singular or the rank of \mathbf{P} equals m or at least m weight functions are non-zero i.e. $n > m$ for each $x \in \Omega$. Substituting Eq. (3.23) into Eq. (3.18), the approximate function $\tilde{U}^k(x)$ can be expressed in terms of the shape functions as

$$\tilde{U}^k(x) = \varphi^T(x) \hat{\mathbf{U}}^k(x) = \sum_{i=1}^n \varphi_i(x) \hat{U}_i^k, \quad \forall x \in \Omega_x, \quad (3.24)$$

where the nodal shape function $\varphi_i(x)$ is given by

$$\varphi^T(x) = \mathbf{p}^T(x) \mathbf{A}^{-1}(x) \mathbf{B}(x),$$

or

$$\varphi_i = \sum_{j=1}^m p_j(x) [\mathbf{A}^{-1}(x) \mathbf{B}(x)]_{ji}. \quad (3.25)$$

Derivatives of $\varphi_i(x)$ are obtained as (see [54, 64, 65] for more details)

$$\begin{aligned} \varphi_{i,x} &= \sum_{j=1}^m p_{j,x} [\mathbf{A}^{-1} \mathbf{B}]_{ji} + p_j [\mathbf{A}^{-1} \mathbf{B}_x + \mathbf{A}_x^{-1} \mathbf{B}]_{ji}, \\ \varphi_{i,xx} &= \sum_{j=1}^m p_{j,xx} [\mathbf{A}^{-1} \mathbf{B}]_{ji} + 2p_{j,x} [\mathbf{A}^{-1} \mathbf{B}_x + \mathbf{A}_x^{-1} \mathbf{B}]_{ji} + p_j [2\mathbf{A}_x^{-1} \mathbf{B}_x + \mathbf{A}^{-1} \mathbf{B}_{xx} + \mathbf{A}_{xx}^{-1} \mathbf{B}]_{ji}, \end{aligned}$$

where $\mathbf{A}_x^{-1} = (\mathbf{A}^{-1})_x$ and $\mathbf{A}_{xx}^{-1} = (\mathbf{A}^{-1})_{xx}$ represent the one and two derivatives of the inverse of \mathbf{A} with respect to x , respectively, which are given by

$$\begin{aligned} \mathbf{A}_x^{-1} &= -\mathbf{A}^{-1} \mathbf{A}_x \mathbf{A}^{-1}, \\ \mathbf{A}_{xx}^{-1} &= -\mathbf{A}_x^{-1} \mathbf{A}_x \mathbf{A}^{-1} - \mathbf{A}^{-1} \mathbf{A}_{xx} \mathbf{A}^{-1} - \mathbf{A}^{-1} \mathbf{A}_x \mathbf{A}_x^{-1}, \end{aligned}$$

where $(\cdot)_x$ denotes $\frac{d(\cdot)}{dx}$.

3.4.2. Local radial point interpolation

According to the local point interpolation [48], the value of point interpolation approximation of $U^k(x)$ at any (given) point $x \in \Omega = [0, 1]$ is approximated by interpolation at n nodes x_1, x_2, \dots, x_n (centers) laying in a convenient neighborhood of x i.e. Ω_x . The domain in which these nodes are chosen, whose shape may depend on the point x , is usually referred to as local support domain. Various different local point interpolation approaches can be obtained depending on the functions used to interpolate $U^k(x)$. In this paper we focus our attention onto the so-called local radial point interpolation method (LRPI), which employs a combination of polynomials and radial basis functions.

The function that interpolate $U^k(x)$ for each $x \in \Omega_x$, which we denote by $U_{RBPI}^k(x)$, is obtained as follows:

$$U_{RBPI}^k(x) = \sum_{i=1}^n R_i(x) a_i^k + \sum_{j=1}^m P_j(x) b_j^k, \quad (3.26)$$

where P_1, P_2, \dots, P_m denote the first m monomials in ascending order (i.e. $P_1 = 1, P_2 = x, \dots, P_m = x^{m-1}$) and R_1, R_2, \dots, R_n are n radial functions centered at x_1, x_2, \dots, x_n , respectively. Moreover $a_1^k, a_2^k, \dots, a_n^k, b_1^k, b_2^k, \dots, b_m^k$ are $n + m$ real coefficients that have to be determined.

As far as the radial basis functions R_1, R_2, \dots, R_n are concerned, several choices are possible (see, for example, [66]). In this work we decide to use the Wu's compactly supported radial basis functions

(WCS-RBFs) with C^4 smoothness [59], as they do not involve any free shape parameter (which is not straightforward to choose, see [67, 68, 69, 39, 40]). WCS-RBFs are as follows:

$$R_i(x) = (1 - r_i)_+^6 (6 + 36r_i + 82r_i^2 + 72r_i^3 + 30r_i^4 + 5r_i^5), \quad i = 1, 2, \dots, n, \quad (3.27)$$

where $r_i = |x - x_i|/r_w$ is the distance from node x_i to x , while r_w is the size of support for the radial function $R_i(x)$. Also, $(1 - r_i)_+^6$ is $(1 - r_i)^6$ for $0 \leq r_i < 1$ and zero otherwise.

Note that the monomials P_1, P_2, \dots, P_m are not always employed (if $b_i^k = 0$, $i = 1, 2, \dots, m$, pure RBF approximation is obtained). In the present work, both the constant and the linear monomials are used to augment the RBFs (i.e. we set $m = 2$).

By requiring that the function U_{RBF}^k interpolate U at x_1, x_2, \dots, x_n , we obtain a set of n equations in the $n + m$ unknown coefficients $a_1^k, a_2^k, \dots, a_n^k, b_1^k, b_2^k, \dots, b_m^k$:

$$\sum_{i=1}^n R_i(x_p) a_i^k + \sum_{j=1}^m P_j(x_p) b_j^k = \hat{U}^k(x_p), \quad p = 1, 2, \dots, n, \quad (3.28)$$

where \hat{U}^k are the fictitious nodal nodes. Moreover, in order to uniquely determine U_{RBF}^k , we also impose:

$$\sum_{i=1}^n P_j(x_i) a_i^k = 0, \quad j = 1, 2, \dots, m. \quad (3.29)$$

That is we have the following system of linear equations:

$$\mathbf{G} \begin{bmatrix} \mathbf{a}^k \\ \mathbf{b}^k \end{bmatrix} = \begin{bmatrix} \hat{\mathbf{U}}^k \\ \mathbf{0} \end{bmatrix},$$

where

$$\hat{\mathbf{U}}^k = \begin{bmatrix} \hat{U}_1^k & \hat{U}_2^k & \dots & \hat{U}_n^k \end{bmatrix}^T = \begin{bmatrix} \hat{U}(x_1) & \hat{U}(x_2) & \dots & \hat{U}(x_n) \end{bmatrix}^T, \quad (3.30)$$

$$\mathbf{G} = \begin{bmatrix} \mathbf{R} & \mathbf{P} \\ \mathbf{P}^T & \mathbf{0} \end{bmatrix},$$

$$\mathbf{R} = \begin{bmatrix} R_1(x_1) & R_2(x_1) & \dots & R_n(x_1) \\ R_1(x_2) & R_2(x_2) & \dots & R_n(x_2) \\ \vdots & \vdots & \ddots & \vdots \\ R_1(x_n) & R_2(x_n) & \dots & R_n(x_n) \end{bmatrix},$$

$$\mathbf{P} = \begin{bmatrix} P_1(x_1) & P_2(x_1) & \dots & P_m(x_1) \\ P_1(x_2) & P_2(x_2) & \dots & P_m(x_2) \\ \vdots & \vdots & \ddots & \vdots \\ P_1(x_n) & P_2(x_n) & \dots & P_m(x_n) \end{bmatrix},$$

$$\mathbf{a}^k = [a_1^k \quad a_2^k \quad \dots \quad a_n^k]^T, \quad (3.31)$$

$$\mathbf{b}^k = [b_1^k \quad b_2^k \quad \dots \quad b_m^k]^T. \quad (3.32)$$

Unique solution is obtained if the inverse of matrix \mathbf{R} exists, so that

$$\begin{bmatrix} \mathbf{a}^k \\ \mathbf{b}^k \end{bmatrix} = \mathbf{G}^{-1} \begin{bmatrix} \hat{\mathbf{U}}^k \\ \mathbf{0} \end{bmatrix}.$$

Accordingly, (3.26) can be rewritten as

$$U_{RBPI}^k(x) = \begin{bmatrix} \mathbf{R}^T(x) & \mathbf{P}^T(x) \end{bmatrix} \begin{bmatrix} \mathbf{a}^k \\ \mathbf{b}^k \end{bmatrix},$$

or, equivalently,

$$U_{RBPI}^k(x) = \begin{bmatrix} \mathbf{R}^T(x) & \mathbf{P}^T(x) \end{bmatrix} \mathbf{G}^{-1} \begin{bmatrix} \hat{\mathbf{U}}^k \\ \mathbf{0} \end{bmatrix}. \quad (3.33)$$

Let us define the vector of shape functions:

$$\Phi(x) = \begin{bmatrix} \varphi_1(x) & \varphi_2(x) & \dots & \varphi_n(x) \end{bmatrix},$$

where

$$\varphi_p(x) = \sum_{i=1}^n R_i(x) \mathbf{G}_{i,p}^{-1} + \sum_{j=1}^m P_j(x) \mathbf{G}_{n+j,p}^{-1}, \quad p = 1, 2, \dots, n, \quad (3.34)$$

and $\mathbf{G}_{i,p}^{-1}$ is the (i, p) element of the matrix \mathbf{G}^{-1} . Using (3.34) relations (3.33) are rewritten in the more compact form:

$$U_{RBPI}^k(x) = \Phi(x) \hat{\mathbf{U}}^k, \quad (3.35)$$

or, equivalently,

$$U_{RBPI}^k(x) = \sum_{i=1}^n \hat{U}_i^k \varphi_i(x). \quad (3.36)$$

It can be easily shown that the shape functions (3.34) satisfy the so-called Kronecker property, that is

$$\varphi_i(x_j) = \delta_{ij}, \quad (3.37)$$

where δ_{ij} is the well-known Kronecker symbol, so that essential boundary and final conditions such as those considered in Section 2 (e.g., (2.4), (2.5), (2.16), (2.17)) can be easily imposed. Note also that the derivatives of U_{RBPI}^k (of any order) with respect to x are easily obtained by direct differentiation in (3.36).

3.5. Discretized equations

For implementation of the LBIE and LRPI methods, $N + 1$ regularly nodes x_j , $j = 0, 1, \dots, N$ are chosen in the interval $[0, 1]$ where $x_0 = 0$ and $x_N = 1$. We define $X = \{x_0, x_1, \dots, x_N\}$. Distance between two nodes is defined by $h = x_{i+1} - x_i$, for $i = 0, 1, \dots, N - 1$. It is important to observe that $U^{k+1}(x)$ must be considered as known quantities, since it is approximated at the previous iteration. We want to approximate $U^k(x)$ using radial point interpolation and MLS approximations. Substituting the displacement expression in Eqs. (3.24) and (3.36) into the local weak forms (3.16) and (3.17), respectively, the discrete equation for each interior node is obtained as follows

$$\begin{aligned} & \sum_{j=1}^n \hat{U}_j^{k+1} \int_{\Omega_s^i} (\theta \alpha''(x) - \theta \beta'(x) + \gamma_1) \varphi_j(x) d\Omega + \theta \sum_{j=1}^n \hat{U}_j^{k+1} (\beta(x) - \alpha'(x)) \varphi_j(x) \Big|_{\partial \Omega_s^i} \\ & + \theta \sum_{j=1}^n \hat{U}_j^{k+1} \alpha(x) \varphi_{j,x}(x) \Big|_{\partial \Omega_s^i} \\ & = \sum_{j=1}^n \hat{U}_j^k \int_{\Omega_s^i} ((\theta - 1) \alpha''(x) - (\theta - 1) \beta'(x) + \gamma_2) \varphi_j(x) d\Omega \\ & + (\theta - 1) \sum_{j=1}^n \hat{U}_j^k (\beta(x) - \alpha'(x)) \varphi_j(x) \Big|_{\partial \Omega_s^i} + (\theta - 1) \sum_{j=1}^n \hat{U}_j^k \alpha(x) \varphi_{j,x}(x) \Big|_{\partial \Omega_s^i} \end{aligned} \quad (3.38)$$

and

$$\begin{aligned}
& \sum_{j=1}^n \widehat{U}_j^{k+1} \int_{\Omega_s^i} \left[\frac{\theta}{2} (\alpha''(x) - \beta'(x)) |x - x^i| + \frac{\theta}{2} (\alpha'(x) - \beta(x)) \text{sgn}(x - x^i) + \gamma_1 \right] \varphi_j(x) d\Omega \\
& - \sum_{j=1}^n \widehat{U}_j^{k+1} \int_{\Omega_s^i} \frac{\theta}{2} \alpha(x) \text{sgn}(x - x^i) \varphi_j(x) d\Omega + \frac{\theta}{2} \sum_{j=1}^n \widehat{U}_j^{k+1} \left[|x - x^i| (\beta(x) - \alpha'(x)) \right] \varphi_j(x) \Big|_{\partial\Omega_s^i} \\
& + \frac{\theta}{2} \sum_{j=1}^n \widehat{U}_j^{k+1} \left[|x - x^i| \alpha(x) \right] \varphi_{j,x}(x) \Big|_{\partial\Omega_s^i} \\
& = \sum_{j=1}^n \widehat{U}_j^k \int_{\Omega_s^i} \left[\frac{\theta-1}{2} (\alpha''(x) - \beta'(x)) |x - x^i| + \frac{\theta-1}{2} (\alpha'(x) - \beta(x)) \text{sgn}(x - x^i) + \gamma_1 \right] \varphi_j(x) d\Omega \\
& - \sum_{j=1}^n \widehat{U}_j^k \int_{\Omega_s^i} \frac{\theta-1}{2} \alpha(x) \text{sgn}(x - x^i) \varphi_j(x) d\Omega + \frac{\theta-1}{2} \sum_{j=1}^n \widehat{U}_j^k \left[|x - x^i| (\beta(x) - \alpha'(x)) \right] \varphi_j(x) \Big|_{\partial\Omega_s^i} \\
& + \frac{\theta-1}{2} \sum_{j=1}^n \widehat{U}_j^k \left[|x - x^i| \alpha(x) \right] \varphi_{j,x}(x) \Big|_{\partial\Omega_s^i}. \tag{3.39}
\end{aligned}$$

The matrix forms of the relations (3.38) and (3.39) are respectively as follows

$$\begin{aligned}
& \sum_{j=1}^n \left(\theta \mathbf{A}_{ij} + \gamma_1 \mathbf{B}_{ij} + \theta \mathbf{C}_{ij} + \theta \mathbf{D}_{ij} \right) \widehat{U}_j^{k+1} = \sum_{j=1}^n \left((\theta-1) \mathbf{A}_{ij} + \gamma_2 \mathbf{B}_{ij} \right. \\
& \left. + (\theta-1) \mathbf{C}_{ij} + (\theta-1) \mathbf{D}_{ij} \right) \widehat{U}_j^k, \tag{3.40}
\end{aligned}$$

and

$$\begin{aligned}
& \sum_{j=1}^n \left(\theta \widetilde{\mathbf{A}}_{ij} + \gamma_1 \widetilde{\mathbf{B}}_{ij} - \theta \widetilde{\mathbf{C}}_{ij} + \theta \widetilde{\mathbf{D}}_{ij} + \theta \widetilde{\mathbf{E}}_{ij} \right) \widehat{U}_j^{k+1} = \sum_{j=1}^n \left((\theta-1) \widetilde{\mathbf{A}}_{ij} + \gamma_2 \widetilde{\mathbf{B}}_{ij} \right. \\
& \left. - (\theta-1) \widetilde{\mathbf{C}}_{ij} + (\theta-1) \widetilde{\mathbf{D}}_{ij} + (\theta-1) \widetilde{\mathbf{E}}_{ij} \right) \widehat{U}_j^k, \tag{3.41}
\end{aligned}$$

where

$$\begin{aligned}
& \mathbf{A}_{ij} = \int_{\Omega_s^i} (\alpha''(x) - \beta'(x)) \varphi_j(x) d\Omega, \quad \mathbf{B}_{ij} = \int_{\Omega_s^i} \varphi_j(x) d\Omega, \\
& \mathbf{C}_{ij} = (\beta(x) - \alpha'(x)) \varphi_j(x) \Big|_{\partial\Omega_s^i}, \quad \mathbf{D}_{ij} = \alpha(x) \varphi_{j,x}(x) \Big|_{\partial\Omega_s^i}, \\
& \widetilde{\mathbf{A}}_{ij} = \frac{1}{2} \int_{\Omega_s^i} \left[(\alpha''(x) - \beta'(x)) |x - x^i| + (\alpha'(x) - \beta(x)) \text{sgn}(x - x^i) \right] \varphi_j(x) d\Omega, \\
& \widetilde{\mathbf{B}}_{ij} = \int_{\Omega_s^i} \varphi_j(x) d\Omega, \quad \widetilde{\mathbf{C}}_{ij} = \frac{1}{2} \int_{\Omega_s^i} \alpha(x) \text{sgn}(x - x^i) \varphi_{j,x}(x) d\Omega, \\
& \widetilde{\mathbf{D}}_{ij} = \frac{1}{2} \left[|x - x^i| (\beta(x) - \alpha'(x)) \right] \varphi_j(x) \Big|_{\partial\Omega_s^i}, \quad \widetilde{\mathbf{E}}_{ij} = \frac{1}{2} \left[|x - x^i| \alpha(x) \right] \varphi_{j,x}(x) \Big|_{\partial\Omega_s^i}. \tag{3.42}
\end{aligned}$$

In the LBIE method, it is difficult to enforce the boundary conditions (3.8) for that the shape function constructed by the MLS approximation lacks the delta Kronecker property. In this work, we use the

collocation method to the nodes on the boundary. In fact, at the boundary x_0 and x_N , $U^k(x)$ will be obtained by

$$E = \tilde{U}^k(x_0) = \sum_{j=1}^n \varphi_j(x_0) \hat{U}_j^k, \quad 0 = \tilde{U}^k(x_N) = \sum_{j=1}^n \varphi_j(x_N) \hat{U}_j^k, \quad (3.43)$$

but in LRPIM, using the delta Kronecker property, the boundary conditions (3.8) can be easily imposed. In fact, we have

$$\hat{U}_j^k = \delta_{1j} E, \quad \hat{U}_j^k = 0, \quad j = 1, 2, \dots, n. \quad (3.44)$$

Therefore, we can rewrite the relations (3.41) and (3.43) in LBIE scheme, and also (3.40) and (3.44) in LRPI scheme in the compact forms

$$\mathbf{P} \hat{\mathbf{U}}^k = \mathbf{Q} \hat{\mathbf{U}}^{k+1} + \hat{\mathbf{H}}^k, \quad (3.45)$$

and

$$\mathbf{F} \hat{\mathbf{V}}^k = \mathbf{G} \hat{\mathbf{V}}^{k+1}. \quad (3.46)$$

In these systems, we have

$$\begin{aligned} \hat{\mathbf{U}}^k &= [\hat{U}_0^k \quad \hat{U}_1^k \quad \hat{U}_2^k \quad \dots \quad \hat{U}_N^k]_{1 \times (N+1)}^T, \\ \hat{\mathbf{V}}^k &= [\hat{U}_1^k \quad \hat{U}_2^k \quad \hat{U}_3^k \quad \dots \quad \hat{U}_{N-1}^k]_{1 \times (N-1)}^T, \end{aligned}$$

also in the linear system (3.45), $\hat{\mathbf{H}}^k$ is an $1 \times (N+1)$ vector

$$\hat{\mathbf{H}}^k = [E \quad 0 \quad 0 \quad \dots \quad 0]_{1 \times (N+1)}^T, \quad (3.47)$$

and \mathbf{Q} is the $(N+1) \times (N+1)$ banded matrix with bandwidth $\mathbf{bw} = 2[r_w] + 1$ whose first and last rows contain only zero elements and the other rows are

$$\mathbf{Q}_i = \theta \tilde{\mathbf{A}}_i + \gamma_1 \tilde{\mathbf{B}}_i - \theta \tilde{\mathbf{C}}_i + \theta \tilde{\mathbf{D}}_i + \theta \tilde{\mathbf{E}}_i, \quad i = 1, \dots, N-1,$$

where

$$\tilde{\mathbf{A}}_{ij} = \begin{cases} \text{integration obtained in relation (3.42),} & x_j \in X \cap \Omega_s^i, \\ 0, & \text{otherwise.} \end{cases}$$

The quantities $\tilde{\mathbf{B}}_i$, $\tilde{\mathbf{C}}_i$, $\tilde{\mathbf{D}}_i$ and $\tilde{\mathbf{E}}_i$ are defined analogously. Also \mathbf{P} is the $(N+1) \times (N+1)$ banded matrix with bandwidth \mathbf{bw} (See Figure 1) whose first and last rows given by the first and second of relations (3.43), respectively, and the other rows are

$$\begin{aligned} \mathbf{P}_i &= (\theta - 1) \tilde{\mathbf{A}}_i + \gamma_2 \tilde{\mathbf{B}}_i - (\theta - 1) \tilde{\mathbf{C}}_i + (\theta - 1) \tilde{\mathbf{D}}_i \\ &\quad + (\theta - 1) \tilde{\mathbf{E}}_i, \quad i = 1, \dots, N-1. \end{aligned} \quad (3.48)$$

On the other hand, in the linear system (3.46), we have two banded matrices \mathbf{F} and \mathbf{G} of size $(N-1) \times (N-1)$ with bandwidth $\mathbf{bw} = 2[r_w] + 1$, so that

$$\begin{aligned} \mathbf{G}_i &= \theta \mathbf{A}_i + \gamma_1 \mathbf{B}_i + \theta \mathbf{C}_i + \theta \mathbf{D}_i, \\ \mathbf{F}_i &= (\theta - 1) \mathbf{A}_i + \gamma_2 \mathbf{B}_i + (\theta - 1) \mathbf{C}_i + (\theta - 1) \mathbf{D}_i, \end{aligned}$$

for $i = 1, 2, \dots, N-1$. Finally, in LBIE scheme, combining Eqs. (3.9) and (3.45) leads to the following system:

$$\begin{cases} \mathbf{P} \hat{\mathbf{U}}^k = \mathbf{Q} \hat{\mathbf{U}}^{k+1} + \hat{\mathbf{H}}^k, \\ \hat{\mathbf{U}}^k = \max\{\hat{\mathbf{U}}^k, \hat{\mathbf{\Pi}}\}, \end{cases} \quad (3.49)$$

to be recursively solved for $k = M - 1, M - 2, \dots, 0$, starting from

$$\hat{\mathbf{U}}^M = \hat{\mathbf{\Pi}}, \quad (3.50)$$

where $\hat{\mathbf{\Pi}}$ are obtained from MLS approximation to option's payoff (3.10).

And for LRPI scheme, we find the following iterative system

$$\begin{cases} \mathbf{F}\hat{\mathbf{\Xi}}^k = \mathbf{G}\hat{\mathbf{V}}^{k+1}, \\ \hat{\mathbf{V}}^k = \max\{\hat{\mathbf{\Xi}}^k, \mathbf{\Pi}\}, \end{cases}$$

to be recursively solved for $k = M - 1, M - 2, \dots, 0$, starting from

$$\hat{\mathbf{V}}^M = \mathbf{\Pi} = [\tilde{\zeta}(x_1) \quad \tilde{\zeta}(x_2) \quad \dots \quad \tilde{\zeta}(x_{N-1})]^T. \quad (3.51)$$

Remark 1: Note that the numerical methods proposed in this work require solving at every time step a system of linear equations (systems (3.45) and (3.46)). These highly sparse linear equations can be solved using efficient solution techniques for sparse matrices based on either direct methods or iterative methods. Direct methods, like LU factorization method, can be applied to any non-singular matrix and are well adapted to matrix inversion and solution of linear systems. These methods are especially well suited to solving dense systems with $\mathcal{O}(N^3)$ computational complexity. Direct methods can be impractical if coefficient matrix is large and sparse, because the triangular factors of a sparse matrix usually have many more nonzero elements than itself. So a considerable amount of memory is required and even the solution of the triangular system costs many floating point operations. This necessitates the use of iterative algorithms to preserve the sparsity of the coefficient matrix. The most powerful iterative algorithm of these types is the Bi-conjugate gradient stabilized method (BCGSTAB) developed by Van de Vorst [70] for solving sparse linear systems. Suppose that the final system of equations has the form $\mathbf{Ax} = \mathbf{b}$. This method generates a sequence of approximate solutions $\{\mathbf{x}^{(k)}\}$ and essentially involve the coefficient matrix \mathbf{A} only in the context of matrix-vector multiplication which is relatively inexpensive for a sparse matrix $\mathcal{O}(N(2\mathbf{bw} + 1))$ as compared to a full matrix $\mathcal{O}(N^2)$. It should also be noted that the complexity of BCGSTAB method $\mathcal{O}(2N(2\mathbf{bw} + 1)K)$, where K is the number of iteration of algorithm. We simply observe that complexity of this algorithm is very lower than complexity of direct methods. Note that in all the cases considered, the tolerance number tolerance is selected as 10^{-10} . Convergence was achieved after less than 5 iterations in all cases tested.

Remark 2: The key note in applying the local weak form schemes is computing the local integrals using an accurate numerical integration rule. In the following we consider the well-known numerical integration

rule named Simpson's rule which has a truncate error of order $\mathcal{O}(r_Q^4)$ to \mathbf{A}_{ij} , \mathbf{B}_{ij} , $\tilde{\mathbf{A}}_{ij}$ and $\tilde{\mathbf{C}}_{ij}$:

$$\begin{aligned}
\mathbf{A}_{ij} &= \int_{\Omega_s^i} (\alpha''(x) - \beta'(x)) \varphi_j(x) d\Omega = \int_{x^i - r_Q}^{x^i + r_Q} (\alpha''(x) - \beta'(x)) \varphi_j(x) dx \\
&= \frac{r_Q}{2} \left[(\alpha''(x^i - r_Q) - \beta'(x^i - r_Q)) \varphi_j(x^i - r_Q) + 4(\alpha''(x^i) - \beta'(x^i)) \varphi_j(x^i) \right. \\
&\quad \left. + (\alpha''(x^i + r_Q) - \beta'(x^i + r_Q)) \varphi_j(x^i + r_Q) \right] + \mathcal{O}(r_Q^4), \\
\mathbf{B}_{ij} &= \int_{\Omega_s^i} \varphi_j(x) d\Omega = \int_{x^i - r_Q}^{x^i + r_Q} \varphi_j(x) dx = \frac{r_Q}{2} \left[\varphi_j(x^i - r_Q) + 4\varphi_j(x^i) + \varphi_j(x^i + r_Q) \right] + \mathcal{O}(r_Q^4), \\
\tilde{\mathbf{A}}_{ij} &= \frac{1}{2} \int_{\Omega_s^i} \left[(\alpha''(x) - \beta'(x)) |x - x^i| + (\alpha'(x) - \beta(x)) \text{sgn}(x - x^i) \right] \varphi_j(x) d\Omega \\
&= \frac{r_Q}{4} \left[\left\{ (\alpha''(x^i - r_Q) - \beta'(x^i - r_Q)) r_Q - (\alpha'(x^i - r_Q) - \beta(x^i - r_Q)) \right\} \varphi_j(x^i - r_Q) \right. \\
&\quad \left. + \left\{ (\alpha''(x^i + r_Q) - \beta'(x^i + r_Q)) r_Q + (\alpha'(x^i + r_Q) - \beta(x^i + r_Q)) \right\} \varphi_j(x^i + r_Q) \right] + \mathcal{O}(r_Q^4), \\
\tilde{\mathbf{C}}_{ij} &= \frac{1}{2} \int_{\Omega_s^i} \alpha(x) \text{sgn}(x - x^i) \varphi_{j,x}(x) d\Omega \\
&= \frac{r_Q}{4} \left[-\alpha(x^i - r_Q) \varphi_{j,x}(x^i - r_Q) + \alpha(x^i + r_Q) \varphi_{j,x}(x^i + r_Q) \right] + \mathcal{O}(r_Q^4),
\end{aligned}$$

The Bi-conjugate gradient stabilized method is presented in the following pseudo code:

begin

Set $\mathbf{x}^{(0)} \leftarrow 0$
Compute $\mathbf{r}^{(0)} = \mathbf{b} - \mathbf{A}\mathbf{x}^{(0)}$
Set $\mathbf{p}^{(0)} \leftarrow \mathbf{r}^{(0)}$, $\mathbf{q}^{(0)} \leftarrow 0$, $\mathbf{v}^{(0)} \leftarrow 0$, $\hat{\omega}^{(0)} \leftarrow 1$, $\beta^{(0)} \leftarrow 1$ and $\alpha^{(0)} \leftarrow 1$
repeat $i = 1, 2, \dots$ until $\|\mathbf{r}^{(i)}\|_2 < \text{tolerance} \|\mathbf{r}^{(0)}\|_2$; tolerance = 10^{-10}

$$\begin{aligned}
\hat{\beta}^{(i)} &= \langle \mathbf{p}^{(i-1)}, \mathbf{r}^{(i-1)} \rangle, \\
\omega^{(i)} &= \frac{\hat{\beta}^{(i)} \hat{\omega}^{(i-1)}}{\beta^{(i-1)} \alpha^{(i-1)}}, \\
\beta^{(i-1)} &= \hat{\beta}^{(i)}, \\
\mathbf{q}^{(i)} &= \mathbf{r}^{(i-1)} + \hat{\omega}^{(i)} (\mathbf{q}^{(i-1)} - \alpha^{(i-1)} \mathbf{v}^{(i-1)}), \\
\mathbf{v}^{(i)} &= \mathbf{A} \mathbf{q}^{(i)}, \\
\hat{\omega}^{(i)} &= \frac{\hat{\beta}^{(i)}}{\langle \mathbf{p}^{(i)}, \mathbf{v}^{(i)} \rangle}, \\
\mathbf{s}^{(i)} &= \mathbf{r}^{(i-1)} - \hat{\omega}^{(i)} \mathbf{v}^{(i)}, \\
\mathbf{t}^{(i)} &= \mathbf{A} \mathbf{s}^{(i)}, \\
\alpha^{(i)} &= \frac{\langle \mathbf{t}^{(i)}, \mathbf{s}^{(i)} \rangle}{\langle \mathbf{t}^{(i)}, \mathbf{t}^{(i)} \rangle}, \\
\mathbf{x}^{(i)} &= \mathbf{x}^{(i-1)} + \hat{\omega}^{(i)} \mathbf{q}^{(i)} + \alpha^{(i)} \mathbf{s}^{(i)}, \\
\mathbf{r}^{(i)} &= \mathbf{s}^{(i)} - \alpha^{(i)} \mathbf{t}^{(i)}
\end{aligned}$$

end repeat
 $\mathbf{x} = \mathbf{x}^{(i)}$,

end

3.6. Stability analysis

In this section, we present an analysis of the stability of the LBIE and LRPI schemes. Initially, we consider the LBIE scheme. In this scheme, the solution at any time level can be obtained using Eqs. (3.24) and (3.49)

$$\tilde{\mathbf{U}}^k = \phi \max\{\mathbf{P}^{-1}\mathbf{Q}\phi^{-1}\tilde{\mathbf{U}}^{k+1} + \mathbf{P}^{-1}\hat{\mathbf{H}}^k, \tilde{\mathbf{\Pi}}\}, \quad (3.52)$$

where ϕ is the $(N+1) \times (N+1)$ banded matrix with bandwidth \mathbf{bw} which is easily obtained using the relation (3.24). Then we have

$$\tilde{\mathbf{U}}^k = \phi \hat{\mathbf{U}}^k,$$

and also we have

$$\tilde{\mathbf{\Pi}}^k = \phi \hat{\mathbf{\Pi}}^k.$$

By choosing $k = l$ and using (3.52), we get $\tilde{\mathbf{U}}^l$. Assume that

$$\hat{\mathbf{U}}^l = [\hat{U}_0^l \quad \hat{U}_1^l \quad \hat{U}_2^l \quad \dots \quad \hat{U}_N^l]^T.$$

Also, let \mathbf{U}_e^l be the exact solution at the l th time level with the following components

$$\mathbf{U}_e^l = [U_{e0}^l \quad U_{e1}^l \quad U_{e2}^l \quad \dots \quad U_{eN}^l]^T.$$

It is well-known that for any $i = 0, 1, \dots, N$, \tilde{U}_i^l is either smaller than U_{ei}^l or greater than it i.e.

$$\tilde{U}_i^l < U_{ei}^l, \quad \text{or} \quad \tilde{U}_i^l \geq U_{ei}^l, \quad \forall i = 0, 1, \dots, N.$$

Case 1: Firstly, we consider the vector components of $\tilde{\mathbf{U}}^l$ and \mathbf{U}_e^l which have the following property

$$\tilde{U}_i^l \geq U_{ei}^l,$$

let us define the vectors ${}_1\tilde{\mathbf{U}}^l$ and ${}_1\mathbf{U}_e^l$ as follow

$${}_1\tilde{U}_i^l = \begin{cases} \tilde{U}_i^l, & \tilde{U}_i^l \geq U_{ei}^l, \\ 0, & \text{otherwise,} \end{cases} \quad {}_1U_{ei}^l = \begin{cases} U_{ei}^l, & \tilde{U}_i^l \geq U_{ei}^l, \\ 0, & \text{otherwise.} \end{cases}$$

Eq. (3.52) can be rewritten using the vector ${}_1\tilde{\mathbf{U}}^l$ as follows

$${}_1\tilde{\mathbf{U}}^l = \phi \max\{\mathbf{P}^{-1}\mathbf{Q}\phi^{-1}{}_1\tilde{\mathbf{U}}^{l+1} + \mathbf{M}\mathbf{P}^{-1}\hat{\mathbf{H}}^l, \mathbf{M}\tilde{\mathbf{\Pi}}\}, \quad (3.53)$$

where \mathbf{M} is a $(N+1) \times (N+1)$ matrix

$$\mathbf{M}_{ij} = \begin{cases} 1, & i = j, \text{ and } \tilde{U}_i^l \geq U_{ei}^l, \\ 0, & \text{otherwise.} \end{cases} \quad (3.54)$$

The error \mathbf{E}_1^l at the l th time level is given by

$$\mathbf{E}_1^l = {}_1\tilde{\mathbf{U}}^l - {}_1\mathbf{U}_e^l. \quad (3.55)$$

It is important to observe that all components of \mathbf{E}_1^l are positive values, also we conclude

$${}_1\tilde{\mathbf{U}}^l = \mathbf{E}_1^l + {}_1\mathbf{U}_e^l. \quad (3.56)$$

Using the relations (3.53) and (3.56), we get

$$\mathbf{E}_1^l + {}_1\mathbf{U}_e^l = \phi \max\{\mathbf{P}^{-1}\mathbf{Q}\phi^{-1}{}_1\mathbf{U}_e^{l+1} + \mathbf{M}\mathbf{P}^{-1}\hat{\mathbf{H}}^l + \mathbf{P}^{-1}\mathbf{Q}\phi^{-1}\mathbf{E}_1^{l+1}, \mathbf{M}\tilde{\mathbf{\Pi}}\}, \quad (3.57)$$

we can easily see that the relation (3.57) is transformed to the following equation using the maximum function properties:

$$\begin{aligned} \mathbf{E}_1^l + {}_1\mathbf{U}_e^l &\leq \phi \max\{\mathbf{P}^{-1}\mathbf{Q}\phi^{-1}{}_1\mathbf{U}_e^{l+1} + \mathbf{M}\mathbf{P}^{-1}\hat{\mathbf{H}}^l, \mathbf{M}\tilde{\Pi}\} \\ &\quad + \phi \max\{\mathbf{P}^{-1}\mathbf{Q}\phi^{-1}\mathbf{E}_1^{l+1}, \mathbf{O}\}, \end{aligned} \quad (3.58)$$

where \mathbf{O} is the zero vector. Also we know that

$${}_1\mathbf{U}_e^l = \phi \max\{\mathbf{P}^{-1}\mathbf{Q}\phi^{-1}{}_1\mathbf{U}_e^{l+1} + \mathbf{M}\mathbf{P}^{-1}\hat{\mathbf{H}}^l, \mathbf{M}\tilde{\Pi}\}. \quad (3.59)$$

Therefore, using (3.58) and (3.59) we can write

$$\mathbf{E}_1^l \leq \phi \max\{\mathbf{P}^{-1}\mathbf{Q}\phi^{-1}\mathbf{E}_1^{l+1}, \mathbf{O}\}. \quad (3.60)$$

Finally, we obtain [71]

$$\begin{aligned} \|\mathbf{E}_1^l\| &\leq \|\phi \max\{\mathbf{P}^{-1}\mathbf{Q}\phi^{-1}\mathbf{E}_1^{l+1}, \mathbf{O}\}\| \\ &\leq \|\phi \mathbf{P}^{-1}\mathbf{Q}\phi^{-1}\mathbf{E}_1^{l+1}\| \leq \|\phi \mathbf{P}^{-1}\mathbf{Q}\phi^{-1}\| \|\mathbf{E}_1^{l+1}\|, \end{aligned} \quad (3.61)$$

or, equivalently

$$\|\mathbf{E}_1^l\| \leq \|\phi \mathbf{P}^{-1}\mathbf{Q}\phi^{-1}\| \|\mathbf{E}_1^{l+1}\|. \quad (3.62)$$

Case 2. Now, we consider the vector components of $\tilde{\mathbf{U}}^l$ and \mathbf{U}_e^l which have the following property

$$\tilde{U}_i^l < U_{ei}^l,$$

suppose that ${}_2\tilde{\mathbf{U}}^l$ and ${}_2\mathbf{U}_e^l$ are two vectors defined by

$${}_2\tilde{U}_i^l = \begin{cases} \tilde{U}_i^l, & \tilde{U}_i^l < U_{ei}^l, \\ 0, & \text{otherwise,} \end{cases} \quad {}_2U_{ei}^l = \begin{cases} U_{ei}^l, & \tilde{U}_i^l < U_{ei}^l, \\ 0, & \text{otherwise.} \end{cases}$$

Eq. (3.52) can be rewritten such to contain ${}_2\tilde{\mathbf{U}}^l$ only

$${}_2\tilde{\mathbf{U}}^l = \phi \max\{\mathbf{P}^{-1}\mathbf{Q}\phi^{-1}{}_2\tilde{\mathbf{U}}^{l+1} + \mathbf{N}\mathbf{P}^{-1}\hat{\mathbf{H}}^l, \mathbf{N}\tilde{\Pi}\}, \quad (3.63)$$

where \mathbf{N} is a $(N+1) \times (N+1)$ matrix defined by

$$\mathbf{N}_{ij} = \begin{cases} 1, & i = j, \text{ and } \tilde{U}_i^l < U_{ei}^l, \\ 0, & \text{otherwise.} \end{cases} \quad (3.64)$$

In this case we propose the error \mathbf{E}_2^l at the l th time level

$$\mathbf{E}_2^l = {}_2\tilde{\mathbf{U}}^l - {}_2\mathbf{U}_e^l. \quad (3.65)$$

It is clear that \mathbf{E}_2^l is hold as

$$\mathbf{E}_2^l \geq 0. \quad (3.66)$$

By using relation (3.65), we obtain

$${}_2\tilde{\mathbf{U}}^l = {}_2\mathbf{U}_e^l - \mathbf{E}_2^l. \quad (3.67)$$

Therefore, the relation (3.63) converted to the following equation

$${}_2\mathbf{U}_e^l - \mathbf{E}_2^l = \phi \max\{\mathbf{P}^{-1}\mathbf{Q}\phi^{-1}{}_2\mathbf{U}_e^{l+1} + \mathbf{N}\mathbf{P}^{-1}\hat{\mathbf{H}}^l - \mathbf{P}^{-1}\mathbf{Q}\phi^{-1}\mathbf{E}_2^{l+1}, \mathbf{N}\tilde{\Pi}\}. \quad (3.68)$$

Moreover, using the maximum function property, we have

$$\begin{aligned} {}_2\mathbf{U}_e^l - \mathbf{E}_2^l &\geq \phi \max\{\mathbf{P}^{-1}\mathbf{Q}\phi^{-1}{}_2\mathbf{U}_e^{l+1} + \mathbf{N}\mathbf{P}^{-1}\hat{\mathbf{H}}^l, \mathbf{N}\tilde{\mathbf{\Pi}}\} \\ &\quad - \phi \max\{\mathbf{P}^{-1}\mathbf{Q}\phi^{-1}\mathbf{E}_2^{l+1}, \mathbf{O}\}, \end{aligned} \quad (3.69)$$

or

$$0 \leq \mathbf{E}_2^l \leq \phi \max\{\mathbf{P}^{-1}\mathbf{Q}\phi^{-1}\mathbf{E}_2^{l+1}, \mathbf{O}\}. \quad (3.70)$$

Then, it follows from the norm and maximum property that [71]

$$\begin{aligned} \|\mathbf{E}_2^l\| &\leq \|\phi \max\{\mathbf{P}^{-1}\mathbf{Q}\phi^{-1}\mathbf{E}_2^{l+1}, \mathbf{O}\}\| \leq \|\phi \mathbf{P}^{-1}\mathbf{Q}\phi^{-1}\mathbf{E}_2^{l+1}\| \\ &\leq \|\phi \mathbf{P}^{-1}\mathbf{Q}\phi^{-1}\| \|\mathbf{E}_2^{l+1}\|, \end{aligned} \quad (3.71)$$

or, equivalently

$$\|\mathbf{E}_2^l\| \leq \|\phi \mathbf{P}^{-1}\mathbf{Q}\phi^{-1}\| \|\mathbf{E}_2^{l+1}\|. \quad (3.72)$$

The numerical scheme will be stable if $l \rightarrow \infty$, the error $\|\mathbf{E}_1^l\| \rightarrow 0$ and $\|\mathbf{E}_2^l\| \rightarrow 0$ [71]. This can be guaranteed provided $\rho(\phi \mathbf{P}^{-1}\mathbf{Q}\phi^{-1}) \leq 1$ or $\rho(\mathbf{P}^{-1}\mathbf{Q}) \leq 1$ (because $\mathbf{P}^{-1}\mathbf{Q}$ and $\phi \mathbf{P}^{-1}\mathbf{Q}\phi^{-1}$ are similar matrices), where ρ denotes the spectral radius of the matrix.

For the analysis, we need a simple version of the matrix \mathbf{P} . It is given by

$$\mathbf{P} = (\theta - 1)\tilde{\mathbf{A}} + \gamma_2\tilde{\mathbf{B}} - (\theta - 1)\tilde{\mathbf{C}} + (\theta - 1)\tilde{\mathbf{D}} + (\theta - 1)\tilde{\mathbf{E}} + \mathbf{Z},$$

where $\tilde{\mathbf{A}}, \tilde{\mathbf{B}}, \tilde{\mathbf{C}}, \tilde{\mathbf{D}}$ and $\tilde{\mathbf{E}}$ are the $(N+1) \times (N+1)$ banded matrix with bandwidth \mathbf{bw} whose first and last rows of them contain only zero elements and the other rows are obtain using relation (3.48). Also in the above relation, \mathbf{Z} is an $(N+1) \times (N+1)$ matrix

$$\mathbf{Z}_{ij} = \begin{cases} \varphi_j(x_0), & i = 0, \\ \varphi_j(x_N), & i = N, \\ 0, & \text{otherwise,} \end{cases}$$

where $x_0 = 0$ and $x_N = 1$.

Lemma 1. *In the MLS approximation, if we put*

$$m = 2, \quad r_Q = 0.51h, \quad r_w = 4r_Q,$$

then the following relations hold:

$$\varphi_j(x_0) = \delta_{0j}, \quad \varphi_j(x_N) = \delta_{Nj},$$

where δ is the Kronecker delta.

Proof. We can write the relation (3.25) as follows

$$\varphi_j(x_0) = \sum_{k=1}^2 p_k(0) [\mathbf{A}^{-1}(0)\mathbf{B}(0)]_{kj} = [\mathbf{A}^{-1}(0)\mathbf{B}(0)]_{1j}.$$

Also using section 3.4.1, we have

$$\mathbf{B}(x) = \begin{bmatrix} w_1(x) & w_2(x) & \dots & w_n(x) \\ x_1 w_1(x) & x_2 w_2(x) & \dots & x_n w_n(x) \end{bmatrix},$$

and

$$\mathbf{A}^{-1}(x) = \frac{1}{\begin{bmatrix} \sum_{i=1}^n w_i(x) \\ \sum_{i=1}^n x_i^2 w_i(x) \end{bmatrix} \begin{bmatrix} \sum_{i=1}^n x_i^2 w_i(x) \\ \sum_{i=1}^n x_i w_i(x) \end{bmatrix} - \begin{bmatrix} \sum_{i=1}^n x_i w_i(x) \\ \sum_{i=1}^n w_i(x) \end{bmatrix}^2} \begin{bmatrix} \sum_{i=1}^n x_i^2 w_i(x) & -\sum_{i=1}^n x_i w_i(x) \\ \sum_{i=1}^n x_i w_i(x) & \sum_{i=1}^n w_i(x) \end{bmatrix}.$$

Then, one has

$$[\mathbf{A}^{-1}(0)\mathbf{B}(0)]_{1j} = \frac{w_j(0) \left[\sum_{i=1}^n x_i^2 w_i(0) - x_j \sum_{i=1}^n x_i w_i(0) \right]}{\left[\sum_{i=1}^n w_i(0) \right] \left[\sum_{i=1}^n x_i^2 w_i(0) \right] - \left[\sum_{i=1}^n x_i w_i(0) \right]^2}. \quad (3.73)$$

It is exactly clear that to boundary points x_0 and x_N , we have $n = \lfloor r_w \rfloor + 1$, then here $n = 3$. Indeed, we have $x_j = (j-1)h$, $j = 1, 2, 3$. Eq. (3.73) is calculated as follows

$$[\mathbf{A}^{-1}(0)\mathbf{B}(0)]_{1j} = \frac{w_j(0) \left[\sum_{i=1}^3 (i-1)^2 h^2 w_i(0) - (j-1)h \sum_{i=1}^3 (i-1)h w_i(0) \right]}{\left[\sum_{i=1}^3 w_i(0) \right] \left[\sum_{i=1}^3 (i-1)^2 h^2 w_i(0) \right] - \left[\sum_{i=1}^3 (i-1)h w_i(0) \right]^2}.$$

With a little computation, we conclude that

$$[\mathbf{A}^{-1}(0)\mathbf{B}(0)]_{1j} = \frac{w_j(0) \left[(2-j)w_2(0) + 2(3-j)w_3(0) \right]}{\left[w_1(0)w_2(0) + w_2(0)w_3(0) + 4w_1(0)w_3(0) \right]},$$

on the other hand, we know $w_3(0) = 0$, then

$$[\mathbf{A}^{-1}(0)\mathbf{B}(0)]_{1j} = \frac{(2-j)w_j(0)}{w_1(0)}.$$

Therefore, we obtain

$$\varphi_j(x_0) = [\mathbf{A}^{-1}(0)\mathbf{B}(0)]_{1j} = \delta_{1j}.$$

Now, we want to show $\varphi_j(x_N) = \delta_{Nj}$. Using relation (3.25), we have

$$\varphi_j(x_N) = [\mathbf{A}^{-1}(1)\mathbf{B}(1)]_{1j} + [\mathbf{A}^{-1}(1)\mathbf{B}(1)]_{2j},$$

similar to the above discussion we can claim the following formula

$$[\mathbf{A}^{-1}(1)\mathbf{B}(1)]_{1j} = \frac{w_j(1)[(1-2h)(1-j)w_1(1) + (1-h)(2-j)w_2(1) + (3-j)w_3(1)]}{hw_3(1)(4w_1(1) + w_2(1))},$$

and

$$[\mathbf{A}^{-1}(1)\mathbf{B}(1)]_{2j} = \frac{w_j(1)[(j-1)w_1(1) + (j-2)w_2(1) + (j-3)w_3(1)]}{hw_3(1)(4w_1(1) + w_2(1))}.$$

Also, we get

$$\varphi_j(x_N) = \frac{w_j(1)[2(j-1)w_1(1) + (j-2)w_2(1)]}{w_3(1)(4w_1(1) + w_2(1))}.$$

It is well-known that $w_1(1) = 0$, therefore we have

$$\varphi_j(x_N) = \varphi_j(1) = \delta_{jN}. \quad \square$$

According to Lemma 1 we can write

$$\mathbf{Z}_{ij} = \begin{cases} \delta_{1j}, & i = 0, \\ \delta_{Nj}, & i = N, \\ 0, & \text{otherwise,} \end{cases} \quad (3.74)$$

then we obtain

$$\begin{aligned} \mathbf{P} &= (\theta - 1)\mathbf{S} + \frac{1}{\Delta t}\tilde{\mathbf{B}} + \mathbf{Z}, \\ \mathbf{Q} &= \theta\mathbf{S} + \frac{1}{\Delta t}\tilde{\mathbf{B}}, \end{aligned} \quad (3.75)$$

where

$$\mathbf{S} = \tilde{\mathbf{A}} - r\tilde{\mathbf{B}} - \tilde{\mathbf{C}} + \tilde{\mathbf{D}} + \tilde{\mathbf{E}}.$$

We simply observe that the first and last rows of \mathbf{Q} contain only zero elements, so using Gershgorin theorem all the eigenvalues of \mathbf{Q} are in $\overline{\mathbf{Q}}$, i.e.

$$\mathbf{Q}(x) = \begin{bmatrix} 0 & 0 & \dots & 0 & 0 \\ & & \overline{\mathbf{Q}} & & \\ 0 & 0 & \dots & 0 & 0 \end{bmatrix},$$

where

$$\overline{\mathbf{Q}} = [\mathbf{Q}_2 \quad \mathbf{Q}_3 \quad \dots \quad \mathbf{Q}_N]^T.$$

Also, using the relation (3.74) and (3.75), we can see that

$$\mathbf{P}(x) = \begin{bmatrix} 1 & 0 & \dots & 0 & 0 \\ & & \overline{\mathbf{P}} & & \\ 0 & 0 & \dots & 0 & 1 \end{bmatrix},$$

where

$$\overline{\mathbf{P}} = [\mathbf{P}_2 \quad \mathbf{P}_3 \quad \dots \quad \mathbf{P}_N]^T.$$

It is also worth noticing that one of the eigenvalues of \mathbf{P} is $\lambda = 1$ i.e.

$$\begin{aligned} |\lambda_1 - 1| &\leq 0, & \rightarrow & \lambda_1 = 1, \\ |\lambda_{N+1} - 1| &\leq 0, & \rightarrow & \lambda_{N+1} = 1. \end{aligned}$$

This is obtained using the Gershgorin theorem on the first and last rows of \mathbf{P} . Therefore, the other eigenvalues of \mathbf{P} are in matrix $\overline{\mathbf{P}}$. However, we can consider the $\rho(\overline{\mathbf{P}}^{-1}\overline{\mathbf{Q}})$ instead of $\rho(\mathbf{P}^{-1}\mathbf{Q})$, we have

$$\begin{aligned} \overline{\mathbf{P}} &= (\theta - 1)\overline{\mathbf{S}} + \frac{1}{\Delta t}\overline{\mathbf{B}}, \\ \overline{\mathbf{Q}} &= \theta\overline{\mathbf{S}} + \frac{1}{\Delta t}\overline{\mathbf{B}}, \end{aligned}$$

or

$$\begin{aligned} \overline{\mathbf{B}}^{-1}\overline{\mathbf{P}} &= (\theta - 1)\overline{\mathbf{B}}^{-1}\overline{\mathbf{S}} + \frac{1}{\Delta t}\mathbf{I}, \\ \overline{\mathbf{B}}^{-1}\overline{\mathbf{Q}} &= \theta\overline{\mathbf{B}}^{-1}\overline{\mathbf{S}} + \frac{1}{\Delta t}\mathbf{I}, \end{aligned} \quad (3.76)$$

on the other hand, we know that

$$\overline{\mathbf{P}}^{-1}\overline{\mathbf{Q}} = \overline{\mathbf{P}}^{-1}\overline{\mathbf{B}}\overline{\mathbf{B}}^{-1}\overline{\mathbf{Q}} = (\overline{\mathbf{B}}^{-1}\overline{\mathbf{P}})^{-1}(\overline{\mathbf{B}}^{-1}\overline{\mathbf{Q}}),$$

let us define

$$\mathbf{\Sigma} = \widetilde{\mathbf{B}}^{-1} \overline{\mathbf{P}}, \quad \mathbf{\Gamma} = \widetilde{\mathbf{B}}^{-1} \overline{\mathbf{Q}}, \quad \mathbf{\Upsilon} = \widetilde{\mathbf{B}}^{-1} \overline{\mathbf{S}},$$

therefore, we can rewrite relation (3.77) as follows

$$\begin{aligned} \mathbf{\Sigma} &= (\theta - 1)\mathbf{\Upsilon} + \frac{1}{\Delta t}\mathbf{I}, \\ \mathbf{\Gamma} &= \theta\mathbf{\Upsilon} + \frac{1}{\Delta t}\mathbf{I}. \end{aligned} \tag{3.77}$$

Now by applying Cayley-Hamilton theorem, we have

$$\lambda(\overline{\mathbf{P}}^{-1}\overline{\mathbf{Q}}) = \lambda(\mathbf{\Sigma}^{-1}\mathbf{\Gamma}) = \frac{\lambda(\mathbf{\Gamma})}{\lambda(\mathbf{\Sigma})} = \left| \frac{\theta\Delta t\lambda(\mathbf{\Upsilon}) + 1}{(\theta - 1)\Delta t\lambda(\mathbf{\Upsilon}) + 1} \right| \leq 1, \tag{3.78}$$

where λ are eigenvalues of the matrices. We can easily see that for implicit Euler ($\theta = 0$) and Crank-Nicolson ($\theta = 0.5$) schemes, the inequality (3.78) is always satisfied and the scheme will be unconditionally stable if $\rho(\mathbf{\Upsilon}) \leq 0$. Figure 2 shows numerically how the spectral radius of $\mathbf{\Upsilon}$ varies as a function of N and M . Recollect that the stability condition is satisfied only when $\rho(\mathbf{\Upsilon}) \leq 0$. It can be seen from Figure 2 that this condition is satisfied in the present numerical methods i.e. LBIE and LRPI. In this work, we use Crank-Nicolson scheme which is second-order accuracy with respect to time variable.

Remark 3: Note that the analysis of the stability of the LRPI method is similar to the above analysis. It should also be noted that the stability analysis for European option is similar to the American option.

4. Numerical results and discussions

The numerical simulations are run on a PC Laptop with an Intel(R) Core(TM)2 Duo CPU T9550 2.66 GHz 4 GB RAM and the software programs are written in Matlab. Let U , U_{LBIE} and U_{LRPI} respectively denote the option price (either European or American) and its approximation obtained using the LBIE and LRPI methods developed in the Section 3. To measure the accuracy of the U_{LBIE} and U_{LRPI} methods at the current time ($t = 0$), the discrete maximum norm and the mean square norm have been used with the following definitions:

$$\begin{aligned} \text{MaxError}_{LBIE} &= \max_{i=0,1,\dots,8} |U_{LBIE}(x_i, 0) - U(x_i, 0)|, \\ \text{MaxError}_{LRPI} &= \max_{i=0,1,\dots,8} |U_{LRPI}(x_i, 0) - U(x_i, 0)|, \end{aligned} \tag{4.1}$$

$$\begin{aligned} \text{RMSError}_{LBIE} &= \frac{1}{8+1} \sqrt{\sum_{i=0}^8 (U_{LBIE}(x_i, 0) - U(x_i, 0))^2}, \\ \text{RMSError}_{LRPI} &= \frac{1}{8+1} \sqrt{\sum_{i=0}^8 (U_{LRPI}(x_i, 0) - U(x_i, 0))^2}. \end{aligned} \tag{4.2}$$

In MaxError_{LBIE} , MaxError_{LRPI} , RMSError_{LBIE} and RMSError_{LRPI} , x_i , $i = 0, 1, \dots, 8$ are nine different points that will be chosen in a convenient neighborhood of the strike E , i.e. $x_i \in (\frac{4}{5}E, \frac{6}{5}E)$. For simplicity, in European and American options we set $x_i = 8 + 0.5i$, $i = 0, 1, \dots, 8$ and $x_i = 80 + 5i$, $i = 0, 1, \dots, 8$, respectively. Note that in the case of the American option the exact value of U is not available. Therefore, in (4.1), (4.2) we use instead a very accurate approximation of it, which is obtained using the LBIE method with a very large number of nodes and time steps (precisely we set $N = 1024$ and $M = 1024$).

In the following analysis, the radius of the local sub-domain is selected $r_Q = 0.51h$, where h is the distance between the nodes. The size of r_Q is such that the union of these sub-domain must cover the whole global domain i.e. $\cup \Omega_s^i \subset \Omega$. It is also worth noticing that the MLS approximation is well-defined only when \mathbf{A} is non-singular or the rank of \mathbf{P} equals m or at least m weight functions are non-zero i.e. $n > m$ for each

$x \in \Omega$. Therefore, to satisfy these conditions, the size of the support domain r_w should be large enough to have sufficient number of nodes covered in Ω_x for every sample point ($n > m$). In all the simulations presented in this work we use $r_w = 4r_Q$. Also, in Test cases 1 and 2, we use $\xi = 1$ and $\xi = 0.1$, respectively. These values are chosen by trial and error such as to roughly minimize the errors on the numerical solutions.

To show the rate of convergence of the new schemes when $h \rightarrow 0$ and $\Delta t \rightarrow 0$, the values of ratio with the following formula have been reported in the tables

$$\text{Ratio}_{LBIE} = \log_2 \left\{ \frac{\text{MaxError}_{LBIE} \text{ in the previous row}}{\text{MaxError}_{LBIE} \text{ in the current row}} \right\},$$

$$\text{Ratio}_{LRPI} = \log_2 \left\{ \frac{\text{MaxError}_{LRPI} \text{ in the previous row}}{\text{MaxError}_{LRPI} \text{ in the current row}} \right\}.$$

Finally, the computer time required to obtain the option price using the numerical method described in previous section is denoted by $CPUTime$.

4.1. Test case 1

To test the proposed numerical schemes, our first test problem is the same test problem as is presented in [30] and [72]. To be precise, let us consider an European option with the parameters and option data which are chosen as in Table 1. Moreover, we set $S_{max} = 5E$.

Of special interest to us is testifying the numerical convergence of the solution by this problem. Hence, applying the suggested schemes in this paper together with different choice of N and M , we get the consequences tabulated in Tables 2 and 3. The number of time discretization steps is set equal to nodes distributed in the domain. As we have experimentally checked, this choice is such that in all the simulations performed the error due to the time discretization is negligible with respect to the error due to the LBIE and LRPI discretization (note that in the present work we are mainly concerned with the LBIE and LRPI spatial approximation).

From Tables 2 and 3, it can be seen that the LBIE and LRPI methods provide very accurate, stable and fast approximation for option pricing. We observe that the accuracy grows as the number of basis increases gradually, then the option price can be computed with a small financial error in a small computer time. In fact, for example, in LBIE scheme the option pricing is computed with at least 3 correct significant digits. note that, in Table 2, as well as in the following ones, the fact that MaxError_{LBIE} is approximately 10^{-3} means that $U_{LBIE}(x, 0)$ is up to at least the 3th significant digit, equal to $U(x, 0)$. Moreover, the computer times necessary to perform these simulations are extremely small. In fact, using 32 nodal points in domain and 32 time discretization steps, European option is computed with an error of order 10^{-4} in only 7×10^{-3} second, instead, using 128 nodal points and 128 time discretization steps, the option price is computed with an error of order 10^{-5} in 0.13 second and using 256 nodal points and 256 time discretization steps, the option price is computed with an error of order 10^{-6} in 0.44 second. On the other hand, by looking at Table 3, it can also be seen that in LRPI scheme error of orders 10^{-4} , 10^{-5} and 10^{-6} are computed using 64, 256 and 1024 nodal points and time discretization steps, respectively in 0.01, 0.42 and 7.07 seconds. We can observe that the option price computed by LBIE on sub-domains requires approximately 0.44 second to reach an accuracy of 10^{-6} compared to the 0.42 second required by LRPI method to reach an accuracy of 10^{-5} on the same number of sub-domains. Therefore, we can simply conclude that in this case LBIE method is more accurate than LRPI method. As the final look at the numerical results in Tables 2 and 3, we can see $\frac{\text{MaxError}_{LRPI}}{\text{MaxError}_{LBIE}} \approx 4$, i.e. LBIE scheme is approximately 4 times accurate than LRPI scheme. Also rate of convergence of LBIE is 2 but in LRPI, it is *approximately* 2.

Remark 4: The error estimates of MLS approximation are given in [73] and [74] using different strategies. They have proved that the error of this approximation is of order $\mathcal{O}(\Delta x^m)$. According to theoretical bounds, the ratios should be approximately m . As we can see in Ratio of Table 2, the numerical results confirm the analytical bounds. Anyway, the presented schemes have nearly the order 2 (Note that in previous section we consider $m = 2$).

Comparison with previous works: We can compare the prices obtained from the two meshless methods proposed in this paper with a solution computed in [26]. Hon and his co-author [26] proposed Kansa collocation method combined with method of lines (MOL) for the pricing of European options.

Kansa collocation method is a well-known strong form meshless method based on radial basis functions (especially multi-quadratic radial basis function which is used in [26]) and also the method of lines is a general way of viewing a time-dependent partial differential equation (PDE) as a system of ordinary differential equations (ODEs). The partial derivatives with respect to the space variables are discretized to obtain a system of ODEs in the variable t . This system could be obtained using an explicit fourth order backward time integration scheme (RK4). However, according to what was reported in [26], the numerical proposed therein allows us to obtain the European option price with the $RMSError = 3 \times 10^{-4}$ using $N = 81$ and $M = 30$. In [26], the authors say no any things about the computer time of algorithm but in the other paper of these authors [30], they said that the computer time of Qusi-RBF method for European option pricing which is 12 seconds, is much less than method proposed in [26]. The main reasons of why the our numerical methods are more efficient than the one proposed by [26] are the following: (1) In contrast to the sparse and banded matrices associated with local weak form meshless methods proposed in this paper, the matrices associated to system of the method in [26] usually leads to a fully populated matrices. (2) The approach followed in [26] is based on the MOLs, which allows one to reduce the model to a system of ordinary differential equations (ODEs). However the system of ODEs is solved using RK4 which is a iterative method, in particular, to reach convergence, such an iterative procedure requires us to perform at each time step, a long number of iterations, thus reducing the efficiency of the numerical scheme. However, according to what is reported in this paper, the numerical methods proposed do not have any requirement to solve a system of ODEs. (3) Looking at Tables 2 and 3 and reported result in [26], we can see that the solutions of [26] are slower and more inaccurate than our results. Putting all these things together (comment 2 and this comment), we conclude that the numerical method proposed in this paper is very fast and accurate than the method developed in [26]. (4) More importantly, in [26] there aren't any stability analysis of scheme. (5) The convergence error of approximated solution obtained by [26] is the same as reported by **Remark 4**, i.e. $\mathcal{O}(\Delta x^2)$, but it can be increased using our method by increasing value of m . (please see **Remark 4**).

Let us compare the numerical schemes proposed in this work with that proposed in [30]. Again, in [30], Hon et al. solved this problem using combined MOL method and a strong form meshless method named as Qusi-RBF method. The method is more better than the proposed method in [26], because, the coefficient matrix of the final system is sparse and banded. In [30], the most significant result obtained in Test case 1 is the following: the $RMSError$ is 4×10^{-5} in a computer time 12 seconds using $M = 100$ and $N = 2000$. Let us investigate the reasons why the numerical technique proposed in this paper performs significantly better than the method presented in [30]. (1) The final linear system of our work and [30] is a system using banded coefficient matrix with bandwidth $2P + 1$, but value of P in our work and [30] is 5 and 20, respectively. Therefore, the coefficient matrix obtained using LBIE and LRPI schemes is very more sparse than [30]. (2) In this work, we solve at every time step a sparse and banded linear system using a powerful iterative algorithm named Bi-conjugate gradient stabilized method with complexity $\mathcal{O}(2N(2\mathbf{bw} + 1)K)$, whereas in [30], the authors solved the final linear system with a direct method named banded LU factorization method with partial pivoting with complexity $\mathcal{O}(2NP(P + 2))$. In fact, for example, suppose that in [30] we get $P = 20$ and in our meshless methods we get $\mathbf{bw} = 5$ and $K = 5$. We can easily see that the complexity of [30] is more bigger that our schemes. (3) Authors of [30] did not present the stability analysis for their method. (4) Looking at Tables 2 and 3 and also reported numerical result in [30], we observed that solution of [30] is slower and more inaccurate than our results. In fact, for example, in [30] option price is founded with $RMSError 4 \times 10^{-5}$ in a computer time 12 seconds using $N = 2000$ and $M = 100$, whereas we compute the option price with $RMSError_{LBIE} 3.45 \times 10^{-5}$ in a computer time 0.13 in LBIE using $N = 128$ and $M = 128$ and also $RMSError_{LRPI} 4.37 \times 10^{-5}$ in a computer time 0.42 in LRPI second using $N = 256$ and $M = 256$. Putting all these things together we conclude that the numerical methods proposed in this paper are at least thirty of times faster and more efficient than the method of [30].

4.2. Test case 2

For the second test problem consider an American option with the useful data which are provided in the Table 4. As done in Test case 1, we suppose $S_{max} = 5E$. The results of implementing the problem by utilizing the present methods with various number of sub-domains and time discretization steps are shown in Tables 5 and 6. Overall, as already pointed out, following the numerical findings in the different errors, convinces us that the error of the proposed techniques decrease very rapidly as the number of sub-domains in

domain and time discretization steps increase. In fact, for example, in LBIE and LRPI schemes the price of the American option can be computed with 3 correct significant in only 0.87 and 0.92 second, respectively which is excellent and very fast. We emphasize that the ratio shown in Tables 5 and 6 are approximately 1.5 order accuracy instead of second order. This is thanks to the fact that this model is a free boundary problem, therefore its solution is non-smoothness which spoils the accuracy of the spatial approximation (again we have experimentally checked that the time discretization alone is second-order accurate and thus the low rate of convergence is due to the error of the spatial approximation).

Remark 5: We believe that, in this option model we can do a comparison between our schemes and numerical methods proposed in [30] and [26]. First of all, we emphasize that approximately this comparison is substantially analogous with presented comparison between theirs in Test case 1 and requires only minor changes. In particular, looking at Tables 5 and 6 and what is reported in [30] and [26] we simply observe that the numerical methods proposed in this paper perform much better than the numerical methods proposed in [30] and [26]. In fact, for example, the LBIE and LRPI allow us to compute the American option price with the errors 2.08×10^{-3} and 2.02×10^{-3} in 5.13 and 6.49 seconds, respectively (Tables 5 and 6) using $N = 512$ and $M = 512$, whereas, it takes 47 seconds for the quasi-RBF scheme to compute the option price with the error 3.4×10^{-3} using $N = 2000$ and $M = 500$. Putting all these things together, we conclude that the numerical method proposed in this paper is approximately seven times faster than the method developed in [30].

5. Conclusions

In this paper, the weak form meshless methods namely local boundary integral equation method (LBIE) based on moving least squares approximation (MLS) and local radial point interpolation (LRPI) based on Wu's compactly supported radial basis functions (WCS-RBFs), were formulated and successfully applied to price European and American options under the Black-Scholes model.

Overall the numerical achievements that should be highlighted here are as given in the following:

(1) The price of American option is computed by Richardson extrapolation of the price of Bermudan option. In essence the Richardson extrapolation reduces the free boundary problem and linear complementarity problem to a fixed boundary problem which is much simpler to solve. Thus, instead of describing the aforementioned linear complementarity problem or penalty method, we directly focus our attention onto the partial differential equation satisfied by the price of a Bermudan option which is faster and more accurate than other methods.

(2) The infinite space domain is truncated to $[0, S_{max}]$ with a sufficiently large S_{max} to avoid an unacceptably large truncation error. The options' payoffs considered in this paper are non-smooth functions, in particular their derivatives are discontinuous at the strike price. Therefore, to reduce as much as possible the losses of accuracy the points of the trial functions are concentrated in a spatial region close to the strike prices. So, we employ the change of variables proposed by Clarke and Parrott [60].

(3) We used the θ -weighted scheme. Stability analysis of the method is analyzed and performed by the matrix method in the present paper. In fact, according to an analysis carried out in the present paper, the time semi-discretization is unconditionally stable for implicit Euler ($\theta = 0$) and Crank-Nicolson ($\theta = 0.5$) schemes.

(4) Up to now, only strong form meshless methods based on radial basis functions (RBFs) and quasi-RBF have been used for option pricing in mathematical finance field. These techniques yield high levels of accuracy, but have of a very serious drawback such as produce a very ill-conditioned systems and very sensitive to the select of collocation points. Again we do emphasize that in the new methods presented in this manuscript, coefficient matrix of the linear systems are sparse and banded with bandwidth $\mathbf{bw} = 2\lfloor r_w \rfloor + 1$. It should be noted that these coefficient matrices are positive definite.

(5) The present methods are truly a meshless method, which do not need any *element* or *mesh* for both field interpolation and background integration.

(6) Meshless methods using global RBFs such as Gaussian and multiquadric RBFs have a free parameter known as shape parameter. Despite many research works which are done to find algorithms for selecting the optimum values of ϵ [67, 68, 69, 75, 76], the optimal choice of shape parameter is an open problem which is still under intensive investigation. Cheng et al. [67] showed that when ϵ is very small then the RBFs system error is of exponential order but the solution breaks down when ϵ is smaller than the limiting

value. In general, as the value of the shape parameter ϵ decreases, the matrix of the system to be solved becomes highly ill-conditioned. To overcome this drawback of the global RBFs, the local RBFs such as Wu, Wendland and Buhmann compactly supported radial basis functions which are local and stable functions, are proposed which are applied in this work.

(7) In the LBIE method, it is difficult to enforce the boundary conditions for that the shape function constructed by the MLS approximation lacks the delta Kronecker property but in LRPIM, using the delta Kronecker property, the boundary conditions can be easily imposed. In LBIE, we use the collocation method to the nodes on the boundary.

(8) A crucial point in the weak form meshless methods is an accurate evaluation of the local integrals. Based on MLS and RBFs, the nodal trial functions are highly complicated, hence an accurate numerical integration of the weak form is highly difficult. In this work, the numerical integration procedure used is Simpson's rule, which is well-known to be fourth-order accurate.

(9) It should be noted that LBIE and LRPI schemes lead to banded and sparse system matrices. Therefore, we use a powerful iterative algorithm named the Bi-conjugate gradient stabilized method (BCGSTAB) to get rid of this system. Numerical experiments are presented showing that the LBIE and LRPI approaches are extremely accurate and fast.

(10) To demonstrate the accuracy and usefulness of these methods, some numerical examples were presented. For all test cases, the RMSError, MaxError, Ratio and CPU Time of schemes to various nodal points in domain and time discretization steps, were reported. A good agreement between the results for the LBIE and LRPI techniques, and the solutions obtained by other numerical schemes in literature [30] and [26], was observed clearly. The results of our numerical experiments, confirm the validity of the new techniques.

References

References

- [1] F. Black, M. Scholes, The pricing of options and corporate liabilities, *J. Polit. Econ.* 81 (1973) 637–659.
- [2] M. Brennan, E. Schwartz, Finite difference methods and jump processes arising in the pricing of contingent claim: A synthesis, *J. Financ. Quant. Anal.* 13 (1978) 461–474.
- [3] C. Vazquez, An upwind numerical approach for an American and European option pricing model, *Appl. Math. Comput.* 97 (1998) 273–286.
- [4] X. Wu, W. Kong, A highly accurate linearized method for free boundary problems, *Comput. Math. Appl.* 50 (2005) 1241–1250.
- [5] A. Arciniega, E. Allen, Extrapolation of difference methods in option valuation, *Appl. Math. Comput.* 153 (2004) 165–186.
- [6] M. Yousuf, A. Q. M. Khaliq, B. Kleefeld, The numerical approximation of nonlinear Black-Scholes model for exotic path-dependent American options with transaction cost, *I. J. Comput. Math.* 89 (2012) 1239–1254.
- [7] R. Zvan, P. A. Forsyth, K. R. Vetzal, A general finite element approach for PDE option pricing models, Ph.D. thesis, University of Waterloo, Waterloo (1998).
- [8] L. V. Ballestra, C. Sgarra, The evaluation of American options in a stochastic volatility model with jumps: An efficient finite element approach, *Comput. Math. Appl.* 60 (2010) 1571–1590.
- [9] L. V. Ballestra, L. Cecere, A numerical method to compute the volatility of the fractional Brownian motion implied by American options, *Int. J. Appl. Math.* 26 (2013) 203–220.
- [10] P. A. Forsyth, K. R. Vetzal, Quadratic convergence for valuing American options using a penalty method, *SIAM J. Sci. Comput.* 23 (2002) 2095–2122.
- [11] R. Zvan, P. A. Forsyth, K. Vetzal, A Finite Volume approach for contingent claims valuation, *IMA J. Numer. Anal.* 21 (2001) 703–731.
- [12] S. J. Berridge, J. M. Schumacher, An irregular grid approach for pricing high-dimensional American options, *J. Comput. Appl. Math.* 222 (2008) 94–111.
- [13] A. Q. M. Khaliq, D. A. Voss, S. H. K. Kazmi, Adaptive θ -methods for pricing American options, *J. Comput. Appl. Math.* 222 (2008) 210–227.
- [14] A. Q. M. Khaliq, D. A. Voss, S. H. K. Kazmi, A fast high-order finite difference algorithm for pricing American options, *J. Comput. Appl. Math.* 222 (2008) 17–29.
- [15] B. F. Nielsen, O. Skavhaug, A. Tveito, Penalty methods for the numerical solution of American multi-asset option problems, *J. Comput. Appl. Math.* 222 (2008) 3–16.
- [16] J. Zhao, M. Davison, R. M. Corless, Compact finite difference method for American option pricing, *J. Comput. Appl. Math.* 206 (2007) 306–321.
- [17] D. Tangman, A. Gopaul, M. Bhuruth, Numerical pricing of options using high-order compact finite difference schemes, *J. Comput. Appl. Math.* 218 (2008) 270–280.
- [18] B. Hu, J. Liang, L. Jiang, Optimal convergence rate of the explicit finite difference scheme for American option valuation, *J. Comput. Appl. Math.* 230 (2009) 583–599.
- [19] S. Zhang, L. Wang, A fast numerical approach to option pricing with stochastic interest rate, stochastic volatility and double jumps, *Commun. Nonlinear Sci. Numer. Simulat.* 18 (2013) 1832–1839.

- [20] J. C. Cox, S. A. Ross, M. Rubinstein, Option pricing: A simplified approach, *J. Financ. Econ.* 7 (1979) 229–263.
- [21] M. Broadie, J. Detemple, American option valuation: New bounds, approximations, and a comparison of existing methods, *Rev. Financ. Stud.* 9 (1996) 1211–1250.
- [22] M. Gaudenzi, F. Pressacco, An efficient binomial method for pricing American put options, *Decis. Econ. Finance* 4 (2003) 1–17.
- [23] S. L. Chung, C. C. Chang, R. C. Stapleton, Richardson extrapolation techniques for the pricing of American-style options, *J. Futures Markets* 27 (2007) 791–817.
- [24] A. Khaliq, G. Fasshauer, D. Voss, Using meshfree approximation for multi-asset American option problems, *J. Chinese Institute Engineers* 27 (2004) 563–571.
- [25] L. V. Ballestra, G. Pacelli, Pricing European and American options with two stochastic factors: A highly efficient radial basis function approach, *J. Econ. Dyn. Cont.* 37 (2013) 1142–1167.
- [26] Y. C. Hon, X. Mao, A radial basis function method for solving options pricing models, *Financ. Eng.* 8 (1999) 31–49.
- [27] A. Golbabai, D. Ahmadian, M. Milev, Radial basis functions with application to finance: American put option under jump diffusion, *Math. Comp. Modelling* 55 (2012) 1354–1362.
- [28] Z. Wu, Y. C. Hon, Convergence error estimate in solving free boundary diffusion problem by radial basis functions method, *Eng. Anal. Bound. Elem.* 27 (2003) 73–79.
- [29] M. D. Marcozzi, S. Choi, C. S. Chen, On the use of boundary conditions for variational formulations arising in financial mathematics, *App. Math. Comput.* 124 (2003) 197–214.
- [30] Y. C. Hon, A quasi-radial basis functions method for American options pricing, *Comput. Math. Appl.* 43 (2002) 513–524.
- [31] A. Shokri, M. Dehghan, A Not-a-Knot meshless method using radial basis functions and predictor-corrector scheme to the numerical solution of improved Boussinesq equation, *Comput. Phys. Commun.* 181 (2010) 1990–2000.
- [32] M. Dehghan, R. Salehi, A boundary-only meshless method for numerical solution of the Eikonal equation, *Comput. Mech.* 47 (2011) 283–294.
- [33] M. Dehghan, A. Shokri, Numerical solution of the nonlinear Klein-Gordon equation using radial basis functions, *J. Comput. Appl. Math.* 230 (2009) 400–410.
- [34] K. Parand, J. A. Rad, Kansa method for the solution of a parabolic equation with an unknown spacewise-dependent coefficient subject to an extra measurement, *Comput. Phys. Commun.*, (2012) 184 (2013) 582–595.
- [35] S. Kazem, J. A. Rad, K. Parand, Radial basis functions methods for solving Fokker-Planck equation, *Eng. Anal. Bound. Elem.* 36 (2012) 181–189.
- [36] S. Kazem, J. A. Rad, K. Parand, A meshless method on non-Fickian flows with mixing length growth in porous media based on radial basis functions, *Comput. Math. Appl.* 64 (2012) 399–412.
- [37] K. Rashedi, H. Adibi, J. Rad, K. Parand, Application of meshfree methods for solving the inverse one-dimensional Stefan problem, *Eng. Anal. Bound. Elem.* 40 (2014) 1–21.
- [38] A. A. E. F. Saib, D. Y. Tangman, M. Bhuruth, A new radial basis functions method for pricing American options under Merton’s jump-diffusion model, *I. J. Comput. Math.* 89 (2012) 1164–1185.
- [39] L. V. Ballestra, G. Pacelli, A radial basis function approach to compute the first-passage probability density function in two-dimensional jump-diffusion models for financial and other applications, *Eng. Anal. Bound. Elem.* 36 (2012) 1546–1554.

- [40] L. V. Ballestra, G. Pacelli, Computing the survival probability density function in jump-diffusion models: A new approach based on radial basis functions, *Eng. Anal. Bound. Elem.* 35 (2011) 1075–1084.
- [41] M. Dehghan, A. Ghesmati, Numerical simulation of two-dimensional sine-gordon solitons via a local weak meshless technique based on the radial point interpolation method (RPIM), *Comput. Phys. Commun.* 181 (2010) 772–786.
- [42] D. Mirzaei, M. Dehghan, New implementation of MLBIE method for heat conduction analysis in functionally graded materials, *Eng. Anal. Bound. Elem.* 36 (2012) 511–519.
- [43] R. Salehi, M. Dehghan, A generalized moving least square reproducing kernel method, *J. Comput. Appl. Math.* 249 (2013) 120–132.
- [44] R. Salehi, M. Dehghan, A moving least square reproducing polynomial meshless method, *Appl. Numer. Math.* 69 (2013) 34–58.
- [45] M. Dehghan, A. Shokri, Implementation of meshless LBIE method to the 2D non-linear SG problem, , volume 79 (2009) pages 1662–1682 ., *I. J. Numer. Meth. Eng.* 79 (2009) 1662–1682.
- [46] T. Zhu, J. D. Zhang, S. N. Atluri, A local boundary integral equation (LBIE) method in computational mechanics, and a meshless discretization approach, *Comput. Mech.* 21 (1998) 223–235.
- [47] J. Wang, G. Liu, A point interpolation meshless method based on radial basis functions, *Int. J. Numer. Meth. Eng.* 54 (2002) 1623–1648.
- [48] G. Liu, Y. Gu, *An Introduction to Meshfree Methods and Their Programing*, Springer, Netherlands, 2005.
- [49] S. N. Atluri, H. G. Kim, J. Y. Cho, A critical assessment of the truly meshless local Petrov-Galerkin (MLPG), and local boundary integral equation (LBIE) methods, *Comput. Mech.* 24 (1999) 348–372.
- [50] T. Zhu, J. D. Zhang, S. N. Atluri, A meshless local boundary integral equation (LBIE) for solving nonlinear problems, *Comput. Mech.* 22 (1998) 174–186.
- [51] T. Zhu, J. D. Zhang, S. N. Atluri, A meshless numerical method based on the local boundary integral equation (LBIE) to solve linear and non-linear boundary value problems, *Eng. Anal. Bound. Elem.* 23 (1999) 375–389.
- [52] J. Sladek, V. Sladek, C. Zhang, Transient heat conduction analysis in functionally graded materials by the meshless local boundary integral equation method, *Comput. Mat. Sci.* 28 (2003) 494–504.
- [53] J. Sladek, V. Sladek, J. Krivacek, C. Zhang, Local BIEM for transient heat conduction analysis in 3-D axisymmetric functionally graded solids, *Comput. Mech.* 32 (2003) 169–176.
- [54] M. Dehghan, D. Mirzaei, Meshless local boundary integral equation (LBIE) method for the unsteady magnetohydrodynamic (MHD) flow in rectangular and circular pipes, *Comput. Phys. Commun.* 180 (2009) 1458–1466.
- [55] A. Shirzadi, V. Sladek, J. Sladek, A local integral equation formulation to solve coupled nonlinear reaction-diffusion equations by using moving least square approximation, *Eng. Anal. Bound. Elem.* 37 (2013) 8–14.
- [56] S. M. Hosseini, V. Sladek, J. Sladek, Application of meshless local integral equations to two dimensional analysis of coupled non-fick diffusion-elasticity, *Eng. Anal. Bound. Elem.* 37 (2013) 603–615.
- [57] V. Sladek, J. Sladek, Local integral equations implemented by MLS-approximation and analytical integrations, *Eng. Anal. Bound. Elem.* 34 (2010) 904–913.
- [58] X. Li, Meshless galerkin algorithms for boundary integral equations with moving least square approximations, *Appl. Numer. Math.* 61 (2011) 1237–1256.

- [59] Z. Wu, Compactly supported positive definite radial functions, *Adv. Comput. Math.* 4 (1995) 283–292.
- [60] N. Clarke, K. Parrott, Multigrid for American option pricing with stochastic volatility, *Appl. Math. Finance* 6 (1999) 177–195.
- [61] J. C. Hull, *Options, Futures, Other Derivatives*, 7th ed., Prentice Hall, University of Toronto, 2002.
- [62] C. C. Chang, J. B. Lin, W. C. Tsai, Y. H. Wang, Using Richardson extrapolation techniques to price American options with alternative stochastic processes, *Review of quantitative finance and accounting* 39 (2012) 383–406.
- [63] P. Wilmott, J. Dewynne, S. Howison, *Option Pricing: Mathematical Models and Computation*, Oxford Financial Press, 1996.
- [64] M. Dehghan, D. Mirzaei, Meshless local Petrov-Galerkin (MLPG) method for the unsteady magnetohydrodynamic (MHD) flow through pipe with arbitrary wall conductivity, *Appl. Numer. Math* 59 (2009) 1043–1058.
- [65] M. Dehghan, D. Mirzaei, The meshless local Petrov-Galerkin MLPG method for the generalized two-dimensional non-linear Schrodinger equation, *Eng. Anal. Bound. Elem.* 32 (2008) 747–756.
- [66] M. D. Buhmann, *Radial Basis Functions: Theory and Implementations*, Cambridge University Press, New York, 2004.
- [67] A. H. D. Cheng, M. A. Golberg, E. J. Kansa, Q. Zammito, Exponential convergence and H-c multiquadric collocation method for partial differential equations, *Numer. Meth. Part. D. E.* 19 (2003) 571–594.
- [68] R. E. Carlson, T. A. Foley, The parameter r^2 in multiquadric interpolation, *Comput. Math. Appl.* 21 (1991) 29–42.
- [69] G. Fasshauer, J. Zhang, On choosing “optimal” shape parameters for RBF approximation, *Numer. Algorithms* 45 (2007) 346–368.
- [70] H. V. der Vorst, BCGSTAB: a fast and smoothly converging variant of BCG for the solution of non-symmetric linear systems, *SIAM J.Sci. Stat. Comp.* 18 (1992) 631–634.
- [71] B. N. Datta, *Numerical Linear Algebra and Applications*, 2th ed., SIAM, 2010.
- [72] P. Wilmott, S. Howison, J. Dewynne, *The Mathematics of Financial Derivatives*, Cambridge University Press, 1995.
- [73] H. Wendland, *Scattered Data Approximation*, Cambridge University Press, New York, 2005.
- [74] D. Mirzaei, R. Schaback, M. Dehghan, On generalized moving least squares and diffuse derivatives, *IMA J. Numer. Anal.* 32 (2012) 983–1000.
- [75] S. Rippa, An algorithm for selecting a good parameter c in radial basis function interpolation, *Advan. Comp. Math.* 11 (1999) 193–210.
- [76] A. E. Tarwater, A parameter study of Hardy’s multiquadric method for scattered data interpolation, Report UCRL-53670, Lawrence Livermore National Laboratory, 1985.

Table 1: Test case 1, model parameters and data

Volatility	Interest rate	Strike price	Maturity
$0.2 \text{ year}^{-0.5}$	0.05 year^{-1}	10	0.5 year

Table 2: Test case 1, efficiency of the LBIE scheme

N	M	RMSError_{LBIE}	MaxError_{LBIE}	Ratio_{LBIE}	CPU Time (s)
16	16	3.17×10^{-3}	6.94×10^{-3}	—	0.005
32	32	2.42×10^{-4}	5.55×10^{-4}	3.64	0.007
64	64	5.90×10^{-5}	1.38×10^{-4}	2.01	0.02
128	128	1.46×10^{-5}	3.45×10^{-5}	2.00	0.13
256	256	3.61×10^{-6}	8.54×10^{-6}	2.01	0.44
512	512	8.78×10^{-7}	2.10×10^{-6}	2.02	3.79
1024	1024	2.09×10^{-7}	5.06×10^{-7}	2.05	6.34

Table 3: Test case 1, efficiency of the LRPI scheme

N	M	RMSError_{LRPI}	MaxError_{LRPI}	Ratio_{LRPI}	CPU Time (s)
16	16	2.17×10^{-3}	5.70×10^{-3}	—	0.003
32	32	1.11×10^{-3}	2.57×10^{-3}	1.15	0.005
64	64	2.82×10^{-4}	6.54×10^{-4}	1.97	0.01
128	128	7.08×10^{-5}	1.67×10^{-4}	1.97	0.14
256	256	1.77×10^{-5}	4.37×10^{-5}	1.93	0.42
512	512	4.40×10^{-6}	1.18×10^{-5}	1.89	4.11
1024	1024	1.09×10^{-6}	3.42×10^{-6}	1.79	7.07

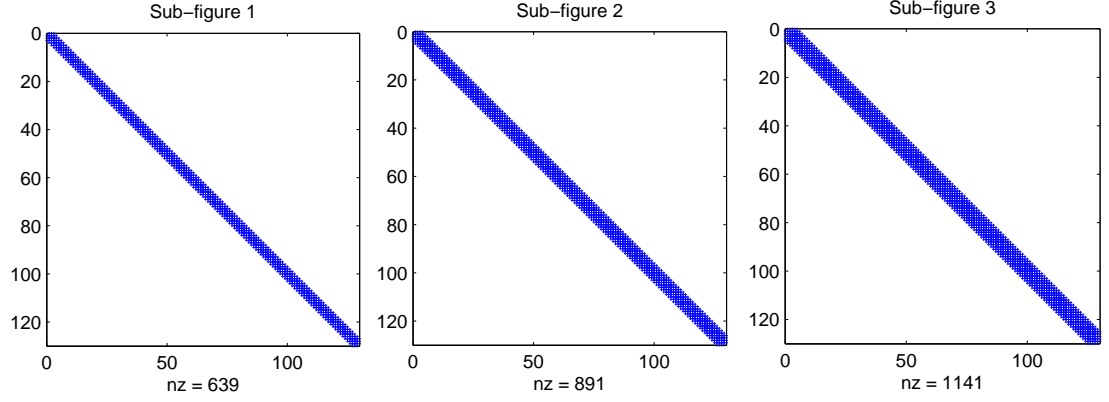


Figure 1: Plot of sparsity for $N = 128$, $r_Q = 0.51h$ and $r_w = 4r_Q$ (sub-figure 1), $r_w = 6r_Q$ (sub-figure 2), $r_w = 8r_Q$ (sub-figure 3)

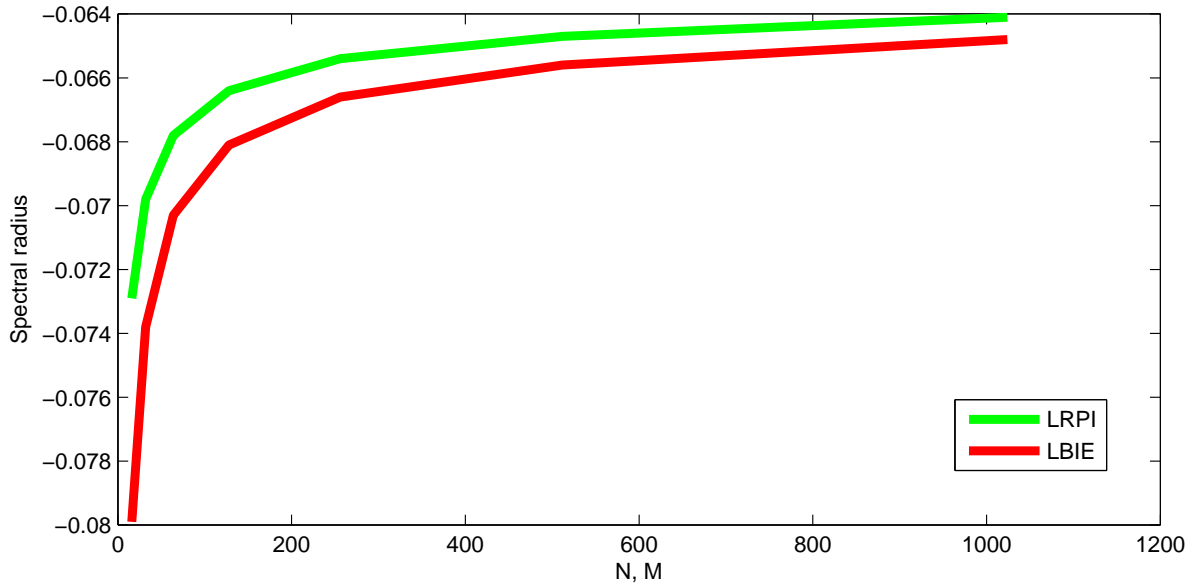


Figure 2: Spectral radius of Υ in LRPI and LBIE methods

Table 4: Test case 2, model parameters and data

Volatility	Interest rate	Strike price	Maturity
$0.3 \text{ year}^{-0.5}$	0.1 year^{-1}	100	1 year

Table 5: Test case 2, efficiency of the LBIE scheme

N	M	RMSError_{LBIE}	MaxError_{LBIE}	Ratio_{LBIE}	CPU Time (s)
64	64	5.79×10^{-3}	3.86×10^{-2}	—	0.05
128	128	2.74×10^{-3}	1.67×10^{-2}	1.21	0.22
256	256	1.19×10^{-3}	6.11×10^{-3}	1.44	0.87
512	512	4.13×10^{-4}	2.08×10^{-3}	1.55	5.13

Table 6: Test case 2, efficiency of the LRPI scheme

N	M	RMSError_{LRPI}	MaxError_{LRPI}	Ratio_{LRPI}	CPU Time (s)
64	64	8.13×10^{-3}	3.15×10^{-2}	—	0.02
128	128	3.49×10^{-3}	1.56×10^{-2}	1.01	0.21
256	256	1.37×10^{-3}	5.75×10^{-3}	1.44	0.92
512	512	4.50×10^{-4}	2.02×10^{-3}	1.51	6.49